

Universal thermodynamics of the one-dimensional attractive Hubbard model

Song Cheng

*State Key Laboratory of Magnetic Resonance and Atomic and Molecular Physics,
Wuhan Institute of Physics and Mathematics, Chinese Academy of Sciences, Wuhan 430071, China
University of Chinese Academy of Sciences, Beijing 100049, China. and
Department of Theoretical Physics, Research School of Physics and Engineering,
Australian National University, Canberra ACT 0200, Australia*

Yi-Cong Yu

*State Key Laboratory of Magnetic Resonance and Atomic and Molecular Physics,
Wuhan Institute of Physics and Mathematics, Chinese Academy of Sciences, Wuhan 430071, China and
University of Chinese Academy of Sciences, Beijing 100049, China.*

M. T. Batchelor

*Centre for Modern Physics, Chongqing University, Chongqing 400044, China
Department of Theoretical Physics, Research School of Physics and Engineering,
Australian National University, Canberra ACT 0200, Australia and
Mathematical Sciences Institute, Australian National University, Canberra ACT 0200, Australia*

Xi-Wen Guan*

*State Key Laboratory of Magnetic Resonance and Atomic and Molecular Physics,
Wuhan Institute of Physics and Mathematics, Chinese Academy of Sciences, Wuhan 430071, China
Department of Theoretical Physics, Research School of Physics and Engineering,
Australian National University, Canberra ACT 0200, Australia and
Center for Cold Atom Physics, Chinese Academy of Sciences, Wuhan 430071, China*

(Dated: October 10, 2018)

The one-dimensional (1D) Hubbard model, describing electrons on a lattice with an on-site repulsive interaction, provides a paradigm for the physics of quantum many-body phenomena. Here by solving the thermodynamic Bethe ansatz equations we study the universal thermodynamics, quantum criticality and magnetism of the 1D attractive Hubbard model. We show that the compressibility and the susceptibility of the Fulde-Ferrell-Larkin-Ovchinnikov (FFLO)-like state obey simple additivity rules at low temperatures, indicating an existence of two free quantum fluids. The magnetic properties, such as magnetization and susceptibility, reveal three physical regions: quantum fluids at low temperatures, a non-Fermi liquid at high temperatures and the quantum fluid to non-Fermi liquid crossover in between. The lattice interaction is seen to significantly influence the nature of the FFLO-like state in 1D. Furthermore, we show that the dimensionless Wilson ratio provides an ideal parameter to map out the various phase boundaries and to characterize the two free fluids of the FFLO-like state. The quantum scaling functions for the thermal and magnetic properties yield the same dynamic critical exponent $z = 2$ and correlation critical exponent $\nu = 1/2$ in the quantum critical region whenever a phase transition occurs. Our results provide a rigorous understanding of quantum criticality and free fluids of many-body systems on a 1D lattice.

PACS numbers: 71.10.Fd, 75.40.Cx, 02.30.Ik

I. INTRODUCTION

How to capture the essential features of many-body physics through a simple model is always of great importance in condensed matter physics. In this regard, the Hubbard model¹ has long provided an active area of research since it was put forward as an instance of a Mott insulator and later considered as a potential high- T_c superconductor. The Hubbard model has thus become a prototypical strongly correlated system which provides rich many-body phenomena, such as a Mott transition, superconductivity, spin-charge separation and a Fulde-Ferrell-Larkin-Ovchinnikov (FFLO) state. However, the Hubbard model, as a simplification of in-

teracting fermions on realistic lattices, can be analytically resolved in neither two-dimensions (2D) nor three-dimensions (3D). The one-dimensional (1D) case within a single band is integrable, firstly solved by Lieb and Wu in terms of the Yang-Baxter equation^{2,3} and the nested Bethe ansatz⁴ (see Ref. 5 for an extensive review). More specifically, since Lieb and Wu's seminal work, the 1D repulsive Hubbard model has been investigated in various aspects, including, but not restricted to, thermodynamic properties in the ground state⁶⁻¹¹, low-lying excitations¹²⁻¹⁹, finite temperature thermodynamics^{16,20-24} and correlation functions²⁵⁻³⁵.

The thermodynamics of the 1D Hubbard model is accessible through two alternative approaches – the thermodynamic Bethe ansatz (TBA) equations²⁰ and the

quantum transfer matrix method³⁶. The former is established on the so-called ‘string hypothesis’ and Yang-Yang grand canonical ensemble approach³⁷, whereas the latter stems from the lattice path integral formulations for the partition function³⁸. In principle, the low-lying excitations can be constructed with the help of the TBA equations in the zero temperature limit and by the logarithm of the Lieb-Wu equations^{16,18,19}. Despite these systematic approaches and other methods employed for the study of the ground state properties^{4,6–11} and low-lying excitations^{12–15,17}, a complete understanding of the universal thermodynamics and quantum criticality of the 1D Hubbard model has not yet been achieved. The key reason for preventing the solution of this problem is the difficulty of finding a suitable generating function for the equation of state at low temperatures.

On the other hand, the correlation functions are also extremely difficult to calculate directly using the Bethe wave function. For a 1D conformally invariant system, the critical exponents determining the power law decay of correlation functions are connected with finite-size corrections to the ground state energy^{39–41}. The 1D repulsive Hubbard model is conformally invariant only in the vicinity of Fermi points. The conformal field theory (CFT) approach provides one method to obtain the asymptotics of correlation functions⁴². The low-lying excitations provide a practicable opportunity for an investigation of long distance asymptotics of correlation functions²⁵, where the finite-size corrections are accessible through the Bethe ansatz method²⁶. However, difficulties involved in the actual calculations of correlation functions usually prevent full access to the many-body correlations^{27–31}.

The mechanism of Cooper pairing in the 1D attractive Hubbard model has attracted attention³² due to the discovery of high-temperature superconductors. In particular, the FFLO-like pair correlation and spin correlations are consequently investigated by various methods, such as density-matrix renormalization group³³, quantum Monte Carlo³⁴ and CFT^{35,43}. The nature of the FFLO-like pair correlation was predicted in expansion dynamics of the attractive Hubbard model trapped in 1D⁴⁴. Very recently, trapping cold atoms on optical lattices becomes a promising method to simulate the many-body physics of the Hubbard model^{45–52}. In particular, ultracold atoms offer an ideal platform for testing results predicted from 1D exactly solvable models⁵⁰.

It is understood that the macroscopic behaviour of 1D materials, such as the spin compound $\text{Cu}(\text{C}_4\text{H}_4\text{N}_2)(\text{NO}_3)_2$ ⁵³ and the heavy fermion material YbNi_4P_2 ⁵⁴, demonstrates a type of 3D Fermi liquid behaviour^{55,56}. The motivation of the present work is to provide understanding of free fluid nature and quantum criticality in the context of the 1D attractive Hubbard model. Firstly, the 1D attractive Hubbard model plays an important role in understanding many-body phenomena such as superconductivity, BEC-BCS crossover and FFLO-like correlation³³, with several publications

touching upon it^{6,9,11,17–19,22,24,32}. Secondly, one expects to find universal behaviour for this model, including thermodynamics, quantum criticality and Luttinger liquid properties. Thirdly, regarding the complicated FFLO state, it is highly desirable to obtain simple rules to describe the nature of quantum liquids in the attractive Hubbard model. Last, but not least, the interplay of this work with experiments with ultracold atoms^{45–52} may broaden our knowledge of many-body physics through 1D exactly solvable models.

This paper is organized as follows. In section II, we present a derivation of the TBA equations for the 1D attractive Hubbard model and determine the ground state phase diagram. In section III, we derive the equation of state in the strong coupling regime. In section IV, using the equation of state, we obtain various analytical results for the thermodynamics and magnetism which are relevant to experimental study. We also investigate quantum criticality and obtain the universal scaling forms of thermodynamic quantities. In section V, we demonstrate the free fluid nature of the FFLO phase through the simple additivity rules of the thermodynamic quantities. We find that the compressibility Wilson ratio is very powerful in identifying the Fermi liquid/Tomonaga-Luttinger liquid phases in the low temperature phase diagram. The last section VI is reserved for a summary and conclusion.

We conclude this section by noting that this article provides a fuller and more detailed account of our key results presented elsewhere⁵⁷.

II. THERMODYNAMICS: THE YANG-YANG APPROACH

A. Thermodynamic Bethe Ansatz equations

The 1D Hubbard model is described by the Hamiltonian

$$H = - \sum_{j=1}^L \sum_{a=\uparrow,\downarrow} \left(c_{j,a}^\dagger c_{j+1,a} + c_{j+1,a}^\dagger c_{j,a} \right) + u \sum_{j=1}^L (1 - 2n_{j,\uparrow})(1 - 2n_{j,\downarrow}), \quad (1)$$

where $c_{j,a}^\dagger$ and $c_{j,a}$ are the creation and annihilation operators of fermions with spin a ($a = \uparrow$ or $a = \downarrow$) at site j in a 1D periodic lattice of length L , $n_{j,a} = c_{j,a}^\dagger c_{j,a}$ is the corresponding particle number operator, and u represents an on-site interaction between particles ($u > 0$ for repulsion and $u < 0$ for attraction). By means of the Bethe ansatz, the eigenenergies of the Hamiltonian are given by $E = -2 \sum_{j=1}^N \cos k_j + u(L - 2N)$, where the quasimomenta $\{k_j\}$ satisfy the Lieb-Wu equations⁴

$$\exp(ik_j L) = \prod_{\alpha=1}^M \frac{\sin k_j - \Lambda_\alpha + i u}{\sin k_j - \Lambda_\alpha - i u}, \quad (2)$$

$$\prod_{j=1}^N \frac{\sin k_j - \Lambda_\beta + i u}{\sin k_j - \Lambda_\beta - i u} = - \prod_{\alpha=1}^M \frac{\Lambda_\alpha - \Lambda_\beta + 2 i u}{\Lambda_\alpha - \Lambda_\beta - 2 i u}, \quad (3)$$

where $\{\Lambda_\beta\}$ denote spin rapidities, $j = 1, 2, \dots, N$, $\beta = 1, \dots, M$, with N and M the total particle number and spin down particle number, respectively.

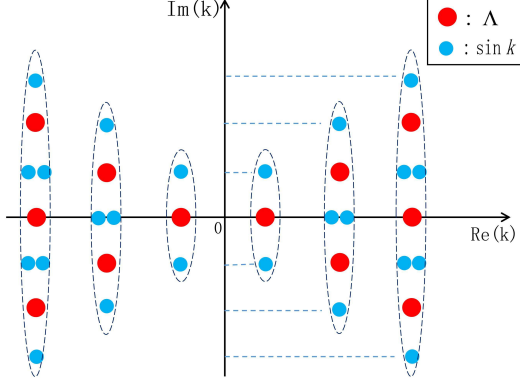


FIG. 1: A schematic configuration of the k - Λ strings of length-1, 2, 3. The k - Λ bound states are formed by the charge momenta and spin rapidities displayed within the dashed boundaries. In each k - Λ bound state $\sin k$'s share a real part with the spin rapidities. A length- m k - Λ string contains m rapidities in Λ -space and $2m$ quasimomenta in k -space. In contrast to the two component Fermi gas, many electrons on a 1D lattice are allowed to form a bound state of multiparticles.

Similar to the analysis²⁰ used for the repulsive case $u > 0$, one finds that the roots to the Bethe ansatz equations (2) and (3) for the attractive Hubbard model can be divided into three categories: single real k , $k - \Lambda$ string and $\Lambda - \Lambda$ string, which constitute the string hypothesis. They are given by^{19,22}

• single real k 's.

• the α -th k - Λ string of length- m , for which there are $2m$ k 's,

$$\begin{aligned} k_\alpha^1 &= \arcsin(\Lambda'_\alpha{}^m + i m |u|), \\ k_\alpha^2 &= \arcsin(\Lambda'_\alpha{}^m + i(m-2)|u|), \\ k_\alpha^3 &= \pi - k_\alpha^2, \\ &\vdots \\ k_\alpha^{2m-2} &= \arcsin(\Lambda'_\alpha{}^m - i(m-2)|u|), \\ k_\alpha^{2m} &= \arcsin(\Lambda'_\alpha{}^m - i m |u|), \end{aligned} \quad (4)$$

accompanied by m spin-rapidities

$$\Lambda_\alpha^{m,j} = \Lambda'_\alpha{}^m + i(m+1-2j)|u|, \quad (5)$$

in Λ space, where $j = 1, 2, 3, \dots, m$ and $\Lambda'_\alpha{}^m$ is the real center of the $k - \Lambda$ string, see Fig. 1.

• the β -th Λ - Λ string of length- m ,

$$\Lambda_\beta^{m,j} = \Lambda_\beta^m + i(m+1-2j)|u|, \quad (6)$$

where $j = 1, 2, 3, \dots, m$, and Λ_α^m is the real center of the Λ string. The Λ strings represent the spin wave bound states in the spin sector.

In the above equations we denoted M_m , M'_m , and \mathcal{M}_e as the number of Λ strings of length m , of k - Λ strings of length- m , and of single real k 's, respectively. It is easy to see that $M = \sum_{m=1}^{\infty} m(M_m + M'_m)$ and $N = \mathcal{M}_e + \sum_{m=1}^{\infty} 2mM'_m$.

Substituting the string hypothesis into the Lieb-Wu equations and taking logarithms leads to the discrete nested BA equations

$$k_j L = 2\pi I_j + \sum_{m=1}^{\infty} \sum_{\alpha=1}^{M'_m} \theta\left(\frac{\sin k_j - \Lambda'_\alpha{}^m}{m|u|}\right) + \sum_{m=1}^{\infty} \sum_{\alpha=1}^{M_m} \theta\left(\frac{\sin k_j - \Lambda_\alpha^m}{m|u|}\right), \quad (7)$$

$$\sum_{j=1}^{N-2M'} \theta\left(\frac{\Lambda_\alpha^n - \sin k_j}{n|u|}\right) = 2\pi J_\alpha^n + \sum_{m=1}^{\infty} \sum_{\beta=1}^{M_m} \Theta_{nm}\left(\frac{\Lambda_\alpha^n - \Lambda_\beta^m}{n|u|}\right), \quad (8)$$

$$2L \operatorname{Re}[\arcsin(\Lambda_\alpha'^n + i n |u|)] = 2\pi J_\alpha'^n + \sum_{j=1}^{N-2M'} \theta\left(\frac{\Lambda_\alpha'^n - \sin k_j}{n|u|}\right) + \sum_{m=1}^{\infty} \sum_{\beta=1}^{M'_m} \Theta_{nm}\left(\frac{\Lambda_\alpha'^n - \Lambda_\beta'^m}{|u|}\right), \quad (9)$$

where $M' = \sum_{m=1}^{\infty} m M'_m$ is the total number of Λ 's involved in the k - Λ strings, $\theta(x) = 2 \arctan(x)$, and

$$\Theta_{nm}(x) = \begin{cases} \theta\left(\frac{x}{|n-m|}\right) + 2\theta\left(\frac{x}{|n-m|+2}\right) + \dots + 2\theta\left(\frac{x}{n+m-2}\right) + \theta\left(\frac{x}{n+m}\right) & \text{if } n \neq m \\ 2\theta\left(\frac{x}{2}\right) + 2\theta\left(\frac{x}{4}\right) + \dots + 2\theta\left(\frac{x}{2n-2}\right) + \theta\left(\frac{x}{2n}\right) & \text{if } n = m. \end{cases} \quad (10)$$

The quantum numbers I_j , J_α^n and $J_\alpha'^n$ are either integers or half-odd integers, stemming from the multivaluedness

of the log functions. They are determined by the relations

$$I_j = \begin{cases} \text{integers} & \text{if } \sum_{m=1}^{\infty} (M'_m + M_m) \text{ is even} \\ \text{half-odd integers} & \text{if } \sum_{m=1}^{\infty} (M'_m + M_m) \text{ is odd,} \end{cases}$$

$$J_\alpha^n = \begin{cases} \text{integers} & \text{if } N - M_n \text{ is odd} \\ \text{half-odd integers} & \text{if } N - M_n \text{ is even,} \end{cases}$$

$$J_\alpha'^n = \begin{cases} \text{integers} & \text{if } L - N + M'_n \text{ is odd} \\ \text{half-odd integers} & \text{if } L - N + M'_n \text{ is even.} \end{cases}$$

With the help of the string hypothesis, the eigenenergies are

$$E = -2 \sum_{j=1}^{N-2M'} \cos k_j - 2uN + uL \quad (11)$$

$$-4 \sum_{n=1}^{\infty} \sum_{\alpha=1}^{M'_n} \text{Re} \left[\sqrt{1 - (\Lambda_\alpha'^n + i n |u|)^2} \right].$$

We now introduce counting functions for the quantum numbers, $y(k_j) = 2\pi I_j/L$, $z_n(\Lambda_\alpha^n) = 2\pi J_\alpha^n/L$ and $z'_n(\Lambda_\alpha'^n) = 2\pi J_\alpha'^n/L$. Considering the thermodynamic limit, $N, M, L \rightarrow \infty$ with $N/L, M/L$ finite, we further define the distributions

$$\frac{dy(k)}{dk} = 2\pi [\rho^p(k) + \rho^h(k)],$$

$$\frac{dz_n(\Lambda)}{d\Lambda} = 2\pi [\sigma_n^p(\Lambda) + \sigma_n^h(\Lambda)],$$

$$\frac{dz'_n(\Lambda)}{d\Lambda} = 2\pi [\sigma_n'^p(\Lambda) + \sigma_n'^h(\Lambda)],$$

where $\rho^p, \sigma_n^p, \sigma_n'^p$ ($\rho^h, \sigma_n^h, \sigma_n'^h$) are root densities of particles (holes) in quasimomenta of excess fermions, Λ -string parameter space and $k - \Lambda$ string space, respectively. Then one can derive the densities of excess fermions, Λ -spin strings and $k - \Lambda$ strings, with

$$\rho^p(k) + \rho^h(k) = \frac{1}{2\pi} \quad (12)$$

$$- \cos k \sum_{n=1}^{\infty} \int_{-\infty}^{\infty} d\Lambda a_n(\sin k - \Lambda) [\sigma_n^p(\Lambda) + \sigma_n'^p(\Lambda)],$$

$$\sigma_n^h(\Lambda) = \int_{-\pi}^{\pi} dk a_n(\sin k - \Lambda) \rho^p(k)$$

$$- \sum_{m=1}^{\infty} A_{nm} * \sigma_m^p(\Lambda), \quad (13)$$

$$\sigma_n'^h(\Lambda) = \frac{1}{\pi} \text{Re} \left[\frac{1}{\sqrt{1 - (\Lambda + i n |u|)^2}} \right] \quad (14)$$

$$- \sum_{m=1}^{\infty} A_{nm} * \sigma_m'^p(\Lambda) - \int_{-\pi}^{\pi} dk a_n(\sin k - \Lambda) \rho^p(k),$$

where the function

$$a_n(x) = \frac{1}{2\pi} \frac{2n|u|}{(n|u|)^2 + x^2}.$$

As usual, $*$ stands for the convolution $(f * g)(\Lambda) = \int_{-\infty}^{\infty} f(\Lambda - \Lambda')g(\Lambda')d\Lambda'$, namely,

$$A_{nm} * f(x) = \delta_{n,m} f(x) + \int_{-\infty}^{\infty} \frac{dy}{2\pi} \frac{d}{dx} \Theta_{nm} \left(\frac{x-y}{|u|} \right) f(y).$$

Here we denoted the derivative of the function Θ_{nm} as

$$\frac{1}{2\pi} \frac{d}{dx} \Theta_{nm}(x) = \begin{cases} a_{|n-m|}(x) + 2a_{|n-m|+2}(x) \\ + \dots + a_{n+m}(x) & \text{if } n \neq m \\ 2a_2(x) + 2a_4(x) + \dots \\ + 2a_{2n-2}(x) + a_{2n}(x) & \text{if } n = m. \end{cases}$$

The root distribution functions (12)-(14) determine spin and charge excitations, spin dynamics and full energy spectra. In the grand canonical ensemble, the Gibbs free energy per site can be expressed in terms of these root densities in different sectors

$$f = e - \mu n_c - 2Bm - Ts$$

$$= \int_{-\pi}^{\pi} dk (-2 \cos k - \mu - 2u - B) \rho^p(k)$$

$$- \sum_{n=1}^{\infty} \int_{-\infty}^{\infty} d\Lambda \sigma_n'^p(\Lambda) \left[4 \text{Re} \sqrt{1 - (\Lambda_\alpha'^n + i n |u|)^2} \right. \\ \left. + n(2\mu + 4u) \right]$$

$$+ \sum_{n=1}^{\infty} \int_{-\infty}^{\infty} d\Lambda 2n B \sigma_n^p(\Lambda) - Ts + u, \quad (15)$$

where μ is the chemical potential, B the magnetic field and T the temperature. In the above equations n_c is the particle density, $m = \frac{N-2M}{2L}$ the magnetization and s the entropy per site.

Following the Yang-Yang grand canonical description³⁷, the entropy per site is explicitly given by

$$s = \int_{-\pi}^{\pi} dk \left\{ (\rho^p(k) + \rho^h(k)) \ln (\rho^p(k) + \rho^h(k)) - \rho^p(k) \ln \rho^p(k) - \rho^h(k) \ln \rho^h(k) \right\}$$

$$+ \sum_{n=1}^{\infty} \int_{-\infty}^{\infty} d\Lambda \left\{ (\sigma_n'^p(\Lambda) + \sigma_n^h(\Lambda)) \ln (\sigma_n'^p(\Lambda) + \sigma_n^h(\Lambda)) - \sigma_n'^p(\Lambda) \ln \sigma_n'^p(\Lambda) - \sigma_n^h(\Lambda) \ln \sigma_n^h(\Lambda) \right\}$$

$$+ \sum_{n=1}^{\infty} \int_{-\infty}^{\infty} d\Lambda \left\{ \left(\sigma_n^p(\Lambda) + \sigma_n^h(\Lambda) \right) \ln \left(\sigma_n^p(\Lambda) + \sigma_n^h(\Lambda) \right) - \sigma_n^p(\Lambda) \ln \sigma_n^p(\Lambda) - \sigma_n^h(\Lambda) \ln \sigma_n^h(\Lambda) \right\}. \quad (16)$$

In the following, we only consider the physics with $B \geq 0$ and $\mu \leq 0$.

In the thermodynamic equilibrium, the true equilibrium state can be determined by the minimization of the free energy with respect to the densities. Carrying out a variation of (15) under the restriction of (12)-(14), we obtain the TBA equations for the attractive Hubbard model in the form

$$\begin{aligned} \varepsilon^u(k) &= -2 \cos k - \mu - 2u - B \\ &+ \sum_{n=1}^{\infty} \int_{-\infty}^{\infty} d\Lambda a_n (\sin k - \Lambda) \varepsilon_n'^-(\Lambda) \\ &- \sum_{n=1}^{\infty} \int_{-\infty}^{\infty} d\Lambda a_n (\sin k - \Lambda) \varepsilon_n^-(\Lambda), \end{aligned} \quad (17)$$

$$\begin{aligned} \varepsilon_n(\Lambda) &= \int_{-\pi}^{\pi} dk \cos k a_n (\sin k - \Lambda) \varepsilon^{u-}(k) \\ &+ 2nB + \sum_{m=1}^{\infty} T_{nm} * \varepsilon_m^-(\Lambda), \end{aligned} \quad (18)$$

$$\begin{aligned} \varepsilon_n'(\Lambda) &= -4 \operatorname{Re} \sqrt{1 - (\Lambda + i n |u|)^2} - n(2\mu + 4u) \\ &+ \int_{-\pi}^{\pi} dk \cos k a_n (\sin k - \Lambda) \varepsilon^{u-}(k) \\ &+ \sum_{m=1}^{\infty} T_{nm} * \varepsilon_m'^-(\Lambda), \end{aligned} \quad (19)$$

where we have denoted

$$\begin{aligned} \varepsilon^{u-}(x) &= T \ln \left(1 + e^{-\varepsilon^u(x)/T} \right), \\ \varepsilon_n'^-(x) &= T \ln \left(1 + e^{-\varepsilon_n'(x)/T} \right), \\ \varepsilon_n^-(x) &= T \ln \left(1 + e^{-\varepsilon_n(x)/T} \right). \end{aligned}$$

In the above equations, we defined the dressed energies

$$\begin{aligned} \varepsilon^u(k) &= T \ln \zeta(k) = T \ln \rho^h(k) / \rho^p(k), \\ \varepsilon_n(\Lambda) &= T \ln \eta_n(\Lambda) = T \ln \sigma_n^h(\Lambda) / \sigma_n^p(\Lambda), \\ \varepsilon_n'(\Lambda) &= T \ln \eta_n'(\Lambda) = T \ln \sigma_n'^h(\Lambda) / \sigma_n'^p(\Lambda). \end{aligned}$$

The convolution $T_{nm} * f(x) = A_{nm} * f(x) - \delta_{n,m} f(x)$ is defined by convention.

The TBA equations (17)-(19) indicate that the dressed energies $\varepsilon^u(k)$, $\varepsilon_n(\Lambda)$, $\varepsilon_n'(\Lambda)$ describe the excitation energies which are subject to interactions among the bound states of electrons, spin wave fluctuations, magnetic field and chemical potential. They contain full thermal and magnetic fluctuations in both spin and charge degrees of freedom. Therefore from these equations we can determine the thermal and magnetic properties of the model in

full temperature regimes. After some algebra, the Gibbs free energy per site is consequently given by

$$\begin{aligned} f &= u - \int_{-\pi}^{\pi} \frac{dk}{2\pi} \varepsilon^{u-}(k) \\ &- \sum_{n=1}^{\infty} \int_{-\infty}^{\infty} \frac{d\Lambda}{\pi} \operatorname{Re} \left[\frac{1}{\sqrt{1 - (\Lambda + i n |u|)^2}} \right] \varepsilon_n'^-(\Lambda). \end{aligned} \quad (20)$$

This result builds up analytical access to the full thermodynamics of the model.

B. Zero Temperature Phase Diagram

In the zero temperature limit, most dressed energies are nonnegative and thus make no significant contributions to the free energy (20). We observe that in the ground state, there exist only unpaired fermions and bound pairs of fermions. The spin Λ - Λ strings Eq.(18) are suppressed due to the fact that in the FFLO-like phase IV, the spin wave bound states ferromagnetically couple to the Fermi sea of the unpaired fermions. The driving term in the TBA equation (18) is positive due to this ferromagnetic ordering. At $T \rightarrow 0$, the Λ - Λ strings are gapped. The driving term in the TBA equation (19) can be positive when $n \geq 2$ due to the negative chemical potential. Taking the limit $T \rightarrow 0$, the corresponding TBA equations (17) and (19) thus reduce to coupled linear integral equations, called the dressed energy equations,

$$\begin{aligned} \varepsilon^u(k) &= -2 \cos k - \mu - 2u - B \\ &- \int_{-A}^A d\Lambda a_1 (\sin k - \Lambda) \varepsilon_1'(\Lambda), \\ \varepsilon_1'(\Lambda) &= -2\mu - 2 \int_{-\pi}^{\pi} dk \cos^2 k a_1 (\sin k - \Lambda) \\ &- \int_{-Q}^Q dk \cos k a_1 (\sin k - \Lambda) \varepsilon^u(k) \\ &- \int_{-A}^A d\Lambda' a_2 (\Lambda - \Lambda') \varepsilon_1'(\Lambda'), \end{aligned} \quad (21)$$

where the integration boundaries Q and A represent the Fermi points of these two kinds of states (pairs and single fermions). In Eq. (22) we used the expression

$$\begin{aligned} &4 \operatorname{Re} \sqrt{1 - (\Lambda - i n |u|)^2} - 4n|u| \\ &= \int_{-\pi}^{\pi} \frac{dk}{\pi} \frac{\cos^2 k 2n|u|}{(nu)^2 + (\sin k - \Lambda)^2}. \end{aligned}$$

The integration boundaries are determined by $\varepsilon^u(\pm Q) = 0$ and $\varepsilon_1'(\pm A) = 0$. Within the intervals $[-Q, Q]$ and $[-A, A]$, the dressed energies are negative, i.e., $\varepsilon^u(k) \leq 0$

and $\varepsilon'_1(\Lambda) \leq 0$. This means that particle states occupy all vacancies in the two Fermi seas.

With the help of (12)-(14), the root densities for quasi-momentum k and spin rapidity Λ in the k - Λ string of length-1 at zero temperature are expressed as

$$\rho(k) = \frac{1}{2\pi} - \cos k \int_{-A}^A d\Lambda a_1(\sin k - \Lambda) \sigma'_1(\Lambda), \quad (23)$$

$$\begin{aligned} \sigma'_1(\Lambda) = & \frac{1}{\pi} \operatorname{Re} \frac{1}{\sqrt{1 - (\Lambda + i|u|)^2}} - \int_{-Q}^Q dk a_1(\sin k - \Lambda) \rho(k) \\ & - \int_{-A}^A d\Lambda' a_2(\Lambda - \Lambda') \sigma'_1(\Lambda'). \end{aligned} \quad (24)$$

In the grand canonical ensemble, we explicitly write down the above root densities, which satisfy the two conditions $\int_{-Q}^Q dk \rho(k) + 2 \int_{-A}^A d\Lambda \sigma'_1(\Lambda) = N/L$ and $\int_{-A}^A d\Lambda \sigma'_1(\Lambda) = M/L = N_{\downarrow}/L$. Thus the total particle density is given by $n_c = N/L = \int_{-Q}^Q dk \rho(k) + 2 \int_{-A}^A d\Lambda \sigma'_1(\Lambda)$ and the magnetization per site by $m = (N - 2M)/(2L) = \frac{1}{2} \int_{-Q}^Q dk \rho(k)$.

By varying the integration boundaries Q and A , the system possesses different fillings and quantum phases. A phase transition occurs when the dressed energies exactly satisfy $\varepsilon^u(0) = 0$, $\varepsilon^u(\pi) = 0$ or $\varepsilon'_1(0) = 0$. Consequently we can determine five phases, (I) vacuum, (II) fully polarized state, (III) half-filling state, (IV) partially polarized state, i.e., FFLO-like state, (V) fully paired state. The phase boundary between (I) and (V) is determined by $\varepsilon'_1(0) = 0$ together with the condition $Q = 0$. Then the TBA equation (22) leads to the critical field value $\mu_c = 2|u| - 2\sqrt{1+u^2}$. The phase boundary between (I) and (II) and between (II) and (III) are determined by the conditions $A = 0$, $\varepsilon^u(0) = 0$ and by $A = 0$, $\varepsilon^u(\pi) = 0$, respectively. With regard to the boundaries for the FFLO-like phase, the situation is much more subtle. The phase boundary between (II) and (IV) is determined by $\varepsilon'_1(0) = 0$ and $\varepsilon^u(Q) = 0$, while the phase boundary between (IV) and (V) is determined by $\varepsilon^u(0) = 0$ and $\varepsilon'_1(A) = 0$.

The phase boundaries in the ground state phase diagram Fig. 2 are summarized as follows

- (I-V)

$$\mu_{c1} = 2|u| - 2\sqrt{1+u^2}. \quad (25)$$

- (I-II)

$$\mu_{c2} = -B - 2u - 2. \quad (26)$$

- (II-III)

$$\mu_{c3} = 2 - B - 2u. \quad (27)$$

- (II-IV)

$$\mu_{c4} = 2|u| - 2\sqrt{1+u^2}$$

$$- \int_{-Q}^Q dk \cos k a_1(\sin k) [\cos Q - \cos k], \quad (28)$$

$$B_{c4} = 2\sqrt{1+u^2} - 2\cos Q$$

$$- \int_{-Q}^Q dk \cos k a_1(\sin k) [\cos Q - \cos k], \quad (29)$$

with $Q \in [0, \pi]$.

- (IV-V) This phase transition occurs if the critical magnetic field is sufficient to break the bound state of fermions, whose boundary in principle is fixed by

$$\begin{aligned} \varepsilon'_1(\Lambda) = & -2\mu - 2 \int_{-\pi}^{\pi} dk \cos^2 k a_1(\sin k - \Lambda) \\ & - \int_{-A}^A d\Lambda' a_2(\Lambda - \Lambda') \varepsilon'_1(\Lambda'), \end{aligned} \quad (30)$$

$$\varepsilon'_1(A) = 0, \quad (31)$$

$$\mu = -2 - 2u - B - \int_{-A}^A d\Lambda a_1(\Lambda) \varepsilon'_1(\Lambda). \quad (32)$$

When $A \ll 1$, the density for pairs of fermions is low, the phase boundary could be obtained by iteration, i.e., by applying Taylor expansion to (30) with respect to Λ , it can be approximately resolved by iteration. The solution of (31) gives A in terms of μ and B , then we derive the phase boundary by substituting the above results for A into the Eqs. (30) and (32). By iteration, we finally obtain

$$\begin{aligned} \mu_{c5} \approx & 2|u| - B - 2 \\ & + \frac{4\sqrt{2}}{\pi|u|\alpha_1} \left[\mu_{c5} + 2(\sqrt{1+u^2} - |u|) \right]^{\frac{3}{2}}. \end{aligned} \quad (33)$$

Here at low energy physics only length-1 k - Λ strings are involved. From the TBA equations (17)-(19), we may introduce the parameters α_n and β_n to indicate the interacting effect of the length- n k - Λ bound states on a lattice in the low density regime. They are given by

$$\begin{aligned} \alpha_n &= \int_{-\pi}^{\pi} dk \frac{2n|u| \cos^2 k (n^2 u^2 - 3 \sin^2 k)}{\pi(n^2 u^2 + \sin^2 k)^3}, \\ \beta_n &= \int_{-\pi}^{\pi} dk a_n(\sin k). \end{aligned}$$

In general, α_n represents the lattice effect in the length- n k - Λ strings.

Meanwhile, if $A \gg 1$, the phase boundary is given by (A23) and (A29) in Appendix (VII A), where we have used the Wiener-Hopf method to solve the TBA integral equations.

From the dressed energy equations (21) and (22) the complete phase diagram at zero temperature is shown in Fig. 2. This phase diagram was also obtained by the Shiba transformation, which builds up a mapping between repulsive and attractive regions in the ground state

of the Hubbard model⁵. However, once we are concerned with the low temperature thermodynamics, correlation functions and quantum criticality, the Shiba transformation does not work in actual calculations, see the analysis of the ground state properties of the attractive Hubbard model²⁷⁻³¹. This is mainly because the different spin-spin strings, $k - \Lambda$ strings and excess fermions have different cut-off processes (the cut-off strings, see Appendix B) at low temperature physics. For example, the spin fluctuation term (the third term) in the unpaired dressed energy can be safely ignored in the strongly attractive Hubbard model at low temperatures. However, the counterpart of such a spin fluctuation term in the repulsive Hubbard model essentially determines the antiferromagnetic ordering. Even in the repulsive regime, such spin string dynamics, quantum criticality and scaling functions still lack an analytical calculation. The ground state properties of the attractive Hubbard model were initially studied by Woynarovich¹¹. In this paper, using the TBA equations (17)-(19), we obtain exact results for the FFLO pairing correlation, universal thermodynamics and quantum criticality of the 1D attractive Hubbard model. Our study provides a precise understanding of the universal low energy physics of interacting fermions with pairing and depairing on a 1D lattice.

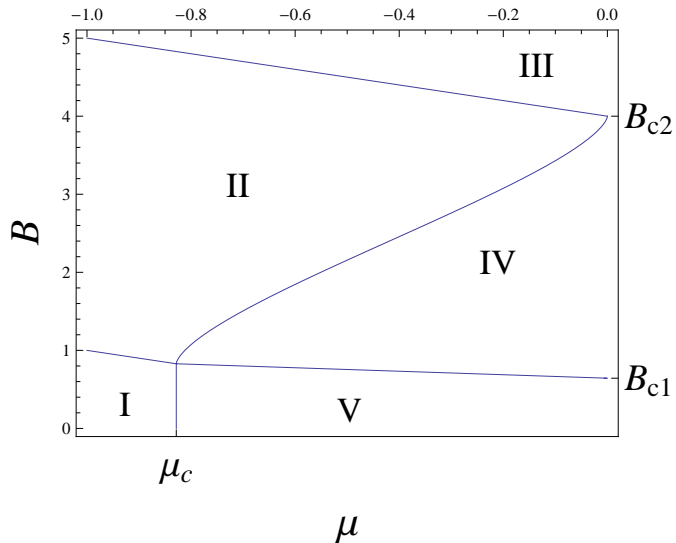


FIG. 2: Ground state phase diagram of the 1D attractive Hubbard model with $|u| = 1$ in the μ - B plane. In the phase diagram, the critical fields are $\mu_c = 2|u| - 2\sqrt{1+u^2} < 0$, $B_{c1} = 2|u| - 2 + 2 \int_{-\infty}^{\infty} d\omega \frac{J_1(\omega) \exp(-|u|\omega)}{w \cosh(u\omega)}$ and $B_{c2} = 2 + 2|u|$. The different phases are denoted by (I) vacuum, (II) fully polarized state, (III) half-filling state, (IV) partially polarized state, (V) fully paired state. The phase boundaries are defined by equations (25)-(33). For comparison the low temperature phase diagram is given in Fig. 9.

III. EQUATION OF STATE

The TBA equations describe the full thermodynamics of the model. At low temperatures quantum liquid behavior and critical scaling in the thermodynamics should be obtained from the TBA equations (17)-(19). However, the analysis of such coupled nonlinear integral equations provides a formidable challenge. In particular, it is challenging to solve infinitely many coupled nonlinear integral TBA equations, i.e., the desired analytical or numerical solution is not achievable by solving the whole set of TBA equations. This obstacle prevents us to understand the microscopic Cooper pairing mechanism and many-body phenomena for this model. On the other hand, in the FFLO-like phase IV, the spin wave bound states ferromagnetically couple to the Fermi sea of the unpaired fermions. In this phase, except two gapless excitations in the sectors of bound pairs and excess fermions, there exist a spin wave ferromagnetic fluctuation, which is no longer a linear dispersion. Bosonization or Tomonaga-Luttinger liquid (TLL) theory⁵⁸ are not available once such a ferromagnetic ordering is involved in the low temperature physics. A similar situation was studied in the 1D two-component Bose gas⁵⁹.

Moreover, the TLL is not applicable to the quantum critical region near a phase transition. Here we proceed with an analytical investigation of the low energy physics of the 1D attractive Hubbard model beyond the scope of the TLL approaches. In order to obtain the universal thermodynamics and quantum criticality of the 1D attractive Hubbard model, we first solve the TBA equations (17)-(19) analytically in the strong coupling regime. We will derive the equation of state which is crucial for the investigation of the quantum criticality of the model. These results can be helpful to understand current experimental developments in ultra-cold atoms⁴⁵⁻⁵⁰.

In the following discussion we mainly concentrate on the low density regime. In general, it is very difficult to find universal characteristics of quantum liquids in quantum many-body systems, for example, for the Gaudin-Yang Fermi gas⁶⁰. Under the assumption that the density of pairs and the bound states of multiple fermions are low and the interaction is strong, the TBA equations (17)-(19) can be rewritten as

$$\varepsilon^u(k) = -2 \cos k + 2\bar{a} \cos^2 k - \mu - 2u - B + \sum_{n=1}^{\infty} p_n^b + \bar{a} - T e^{-2B/T} e^{-\bar{K}} I_0(\bar{K}) + o\left(\frac{1}{|u|^4}\right), \quad (34)$$

$$\varepsilon'_n(\Lambda) = -2n\mu + \eta_n - \frac{d_1}{\pi n|u|} - \frac{d_2}{\pi(n|u|)^3} + \Lambda^2 \left[\frac{d_1}{\pi(n|u|)^3} - \varphi_n \right] + o\left(\frac{1}{|u|^4}\right), \quad (35)$$

where $\bar{K} = \int_{-\pi}^{\pi} \frac{dk}{2\pi} \cos k \ln(1 + e^{-\varepsilon^u(k)/T})$ and $I_0(x)$ is the zeroth order modified Bessel function, which stems from the spin-wave contributions. In the above equations, we

denoted

$$\begin{aligned}
d_1 &= 2\pi - \int_{-\pi}^{\pi} dk \cos k \varepsilon^{u-}(k), \\
d_2 &= -\frac{\pi}{2} - \int_{-\pi}^{\pi} dk \cos k \sin^2 k \varepsilon^{u-}(k), \\
\eta_n &= \sum_{m=1}^{\infty} \int_{-\infty}^{\infty} d\Lambda T_{nm}(\Lambda) \varepsilon'_m{}^-(\Lambda), \\
\bar{a} &= \frac{1}{2} \sum_{n=1}^{\infty} \int_{-\infty}^{\infty} d\Lambda \left[b_n(\Lambda) - \frac{4b_n(\Lambda)\Lambda^2}{(nu)^2 + \Lambda^2} \right] \varepsilon'_n{}^-(\Lambda), \\
\varphi_n &= \sum_{m=1}^{\infty} \int_{-\infty}^{\infty} d\Lambda Q_{nm}(\Lambda) \varepsilon'_m{}^-(\Lambda),
\end{aligned}$$

with $b_n(\Lambda) = \frac{a_n(\Lambda)}{(nu)^2 + \Lambda^2}$ and

$$Q_{nm}(x) = \begin{cases} b_{|n-m|}(x) + 2b_{|n-m|+2}(x) + \dots \\ + 2b_{n+m-2}(x) + b_{n+m}(x) & \text{if } n \neq m \\ 2b_2(x) + 2b_4(x) + \dots \\ + 2b_{2n-2}(x) + b_{2n}(x) & \text{if } n = m. \end{cases} \quad (36)$$

The results (34) and (35) are valid for the low density limit and strong interaction regime.

Substituting Eqs. (34) and (35) into (20), the pressure per unit length is given by $p = p^u + \sum_{n=1}^{\infty} p_n^b + |u|$ with

$$p^u = T \int_{-\pi}^{\pi} \frac{dk}{2\pi} \ln \left(1 + e^{-\varepsilon^u(k)/T} \right), \quad p_n^b = T \int_{-\infty}^{\infty} \frac{d\Lambda}{\pi} \text{Re} \left[\frac{1}{\sqrt{1 - (\Lambda + in|u|)^2}} \right] \ln \left(1 + e^{-\frac{\varepsilon'_n(\Lambda)}{T}} \right). \quad (37)$$

Using the results (34) and (35) and taking integration by parts within the above expressions for the effective pressures (37), we then obtain the set of coupled equations

$$p^u = T \ln \left(1 + e^{(\mu+2u+B-\sum_{n=1}^{\infty} p_n^b + \bar{a}-2)/T} \right) \quad (38)$$

$$\begin{aligned}
& -\frac{2\bar{a}}{\pi} \int_{-1}^1 dx \frac{x^2/\sqrt{1-x^2}}{1+e^{2x/T}/z} + \frac{2\bar{a}}{1+e^{4/T}/z^2} \\
& + \frac{2}{\pi} \int_{-1}^1 dx \frac{\arccos(-x)}{1+e^{2x/T}/z} + o\left(\frac{1}{u^4}\right),
\end{aligned}$$

$$p_n^b = T \left[1 - \frac{1}{4(nu)^2} \right] \ln \left(1 + e^{2n\mu/T} \right) \quad (39)$$

$$\begin{aligned}
& + \frac{2D_n}{\pi} \left[1 - \frac{1}{4(nu)^2} \right] \int_0^{\infty} dx \frac{\arctan \sqrt{x}}{1+e^{D_n x/T}/\zeta_n} \\
& + o\left(\frac{1}{u^4}\right),
\end{aligned}$$

which serve as the equations of state. In the above equations,

$$\begin{aligned}
D_n &= \frac{d_1}{\pi n|u|} - (nu)^2 \varphi_n, \\
z &= e^{(\mu+2u+B-\sum_{n=1}^{\infty} p_n^b + \bar{a})/T}, \\
\zeta_n &= e^{(2n\mu - \eta_n + \frac{d_1}{\pi n|u|} + \frac{d_2}{\pi(n|u|)^3})/T}.
\end{aligned}$$

We also defined the auxiliary functions

$$\begin{aligned}
d_1 &= 2\pi - 4 \int_{-1}^1 dx \frac{\sqrt{1-x^2}}{1+e^{2x/T}/z} \\
& - 4\bar{a} \int_{-1}^1 dx \frac{x^3/\sqrt{1-x^2}}{1+e^{2x/T}/z} + o\left(\frac{1}{u^4}\right), \\
d_2 &= -\frac{\pi}{2} - \frac{4}{3} \int_{-1}^1 dx \frac{(1-x^2)^{3/2}}{1+e^{2x/T}/z} + o\left(\frac{1}{u^4}\right),
\end{aligned}$$

$$\begin{aligned}
\bar{a} &= \sum_{n=1}^{\infty} \frac{D_n}{\pi(nu)^2} \int_0^{\infty} dx \frac{\sqrt{x}/(1+x)^2}{1+e^{D_n x/T}/\zeta_n} + o\left(\frac{1}{u^4}\right), \\
\eta_n &= \sum_{m=1}^{\infty} \mathfrak{T}_{nm}^{\xi}(m) + o\left(\frac{1}{u^4}\right), \\
\varphi_n &= \sum_{m=1}^{\infty} \mathfrak{T}_{nm}^{\phi}(m) + o\left(\frac{1}{u^6}\right). \quad (40)
\end{aligned}$$

In these equations, we define $\mathfrak{T}_{nm}^x(m) = x_{|n-m|}^m + 2x_{|n-m|+2}^m + \dots + 2x_{n+m-2}^m + x_{n+m}^m$, with $x_0^m = 0$ ($x = \eta, \phi$) and auxiliary functions

$$\begin{aligned}
\xi_p^m &= T \ln \left(1 + e^{2m\mu/T} \right) \\
& + \frac{2D_m}{\pi} \int_0^{\infty} dx \frac{\arctan\left(\frac{m}{p}\sqrt{x}\right)}{1+e^{D_m x/T}/\zeta_m}, \\
\phi_p^m &= \frac{T}{2(pu)^2} \left(1 + e^{2m\mu/T} \right) \\
& + \frac{m}{p} \frac{D_m}{\pi u^2} \int_0^{\infty} dx \frac{\sqrt{x}/(p^2 + m^2 x)}{1+e^{D_m x/T}/\zeta_m} \\
& + \frac{D_m}{\pi(pu)^2} \int_0^{\infty} dx \frac{\arctan\left(\frac{m}{p}\sqrt{x}\right)}{1+e^{D_m x/T}/\zeta_m}. \quad (41)
\end{aligned}$$

These functions are indicative of the sophisticated many-body effects induced by k - Λ strings of different lengths. A more detailed derivation of the above result is presented in Appendix VII B.

In order to conceive the universal behavior of the system, we need to further simplify the equations of state (38) and (39). To this end, we utilize the conditions $|\frac{\mu}{T}| \gg 1$ and strong interaction $|u| \gg 1$, which suppress the large length k - Λ strings in this physical regime. We

observe that no larger length- n k - Λ bound states than $n = 1$ exist in the FFLO phase IV at low temperatures. Then the pressure per unit length simplifies to $p = p^u + p^b + |u|$, where p^u and p^b are given by

$$p^u = T \ln \left(1 + e^{(\mu+2u+B-p^b-2)/T} \right) + \frac{2}{\pi} \int_{-1}^1 dx \frac{\arccos(-x)}{1 + e^{2x/T}/z_1} + o\left(\frac{1}{u^2}\right), \quad (42)$$

$$p^b = \frac{2D_1}{\pi} \int_0^\infty dx \frac{\arctan \sqrt{x}}{1 + e^{D_1 x/T}/\zeta} + o\left(\frac{1}{u^2}\right), \quad (43)$$

where $z_1 = e^{(\mu+2u+B-p^b)/T}$, $\zeta = e^{(2\mu-\eta+\frac{d_1}{\pi|u|})/T}$ and the above auxiliary functions with $n = 1$ read

$$D_1 = \frac{d_1}{\pi|u|} - u^2 \varphi, \quad (44)$$

$$d_1 = 2\pi - 4 \int_{-1}^1 dx \frac{\sqrt{1-x^2}}{1 + e^{2x/T}/z_1} + o\left(\frac{1}{u^2}\right), \quad (45)$$

$$\eta = \frac{2D_1}{\pi} \int_0^\infty dx \frac{\arctan(\frac{1}{2}\sqrt{x})}{1 + e^{D_1 x/T}/\zeta} + o\left(\frac{1}{u^2}\right), \quad (46)$$

$$\varphi = \frac{D_1}{2\pi u^2} \int_0^\infty dx \frac{\sqrt{x}/(4+x)}{1 + e^{D_1 x/T}/\zeta} + \frac{D_1}{4\pi u^2} \int_0^\infty dx \frac{\arctan(\frac{1}{2}\sqrt{x})}{1 + e^{D_1 x/T}/\zeta} + o\left(\frac{1}{u^4}\right). \quad (47)$$

Here we only consider the corrections up to order $1/|u|$ in the strong coupling regime $|u| \gg 1$. The equations of state (42) and (43) give a very good approximation of the low energy physics. In Fig. 3, we demonstrate the accuracy of these equations compared to the numerical results obtained from the TBA equations (17)-(19). The peaks in the susceptibility and the discontinuities of the first derivative of the density reveal important behavior of the model near quantum phase transitions.

The pressures (42) and (43) could be further approximately resolved by appropriate iteration. For the low density regime $n_c \ll 1$, we expand the numerators in the pressure p^b and the auxiliary functions η and φ with respect to a small value of x in these integrals. Then we can represent η and φ in terms of p^b . After iteration we thus obtain $p^b \approx -T^{\frac{3}{2}} f_{\frac{3}{2}} / \sqrt{\frac{d_1}{|u|} - \frac{\pi p^b}{8}}$, where we have defined $f_s = \text{Li}_s \left[-\exp\left(\frac{1}{T} \left(2\mu - \frac{p^b}{2} + \frac{d_1}{\pi|u|}\right)\right) \right]$ in terms of the polylog function $\text{Li}_s(x)$. Using this expression for p^b and after some lengthy algebra, we finally obtain the closed form expressions

$$p^b = -\frac{1}{\sqrt{\pi D_0}} T^{\frac{3}{2}} \tilde{f}_{\frac{3}{2}} + o\left(\frac{1}{u^2}, T^2\right), \quad (48)$$

$$p^u = T \ln \left(1 + e^{(\mu+2u+B-p^b-2)/T} \right) + \frac{2}{\pi} \int_{-1}^1 dx \frac{\arccos(-x)}{1 + e^{2x/T}/(z_0 e^{-p^b/T})} + o\left(\frac{1}{u^2}, T^2\right) \quad (49)$$

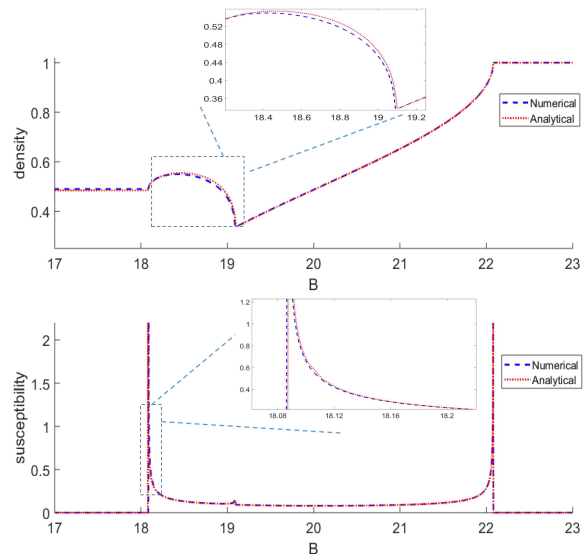


FIG. 3: A comparison between the analytic results (42) and (43) and the numerical results obtained from the TBA equations (17)-(19). We set up natural units in the plots. The upper and the lower panels respectively show the density and susceptibility vs. magnetic field across phases V, IV, II, III at a fixed chemical potential $\mu = -0.08$, temperature $T = 10^{-4}$ and interaction strength $u = -10$. The sudden changes in the density and susceptibility show subtle scaling behavior near phase transitions.

for the two pressures, with the auxiliary functions

$$d_0 = 2\pi - 4 \int_{-1}^1 dx \frac{\sqrt{1-x^2}}{1 + e^{2x/T}/z_0} + o\left(\frac{1}{u^2}, T^2\right), \quad (50)$$

$$D_0 = \frac{d_0}{|u|\pi} + \frac{1}{8} \sqrt{\frac{|u|}{d_0}} T^{\frac{3}{2}} g_{\frac{3}{2}} + o\left(\frac{1}{u^2}, T^2\right). \quad (51)$$

In results (48) and (49), $\tilde{f}_s = g_s - \frac{1}{2} \sqrt{\frac{|u|}{d_0}} T^{\frac{1}{2}} g_s g_{s-1}$, $z_0 = e^{(\mu+2u+B)/T}$ and $g_s = \text{Li}_s \left[-e^{(2\mu+\frac{d_0}{\pi})/T} \right]$. The pressures (48) and (49) give deep insight into quantum scaling in the critical regimes.

IV. QUANTUM CRITICALITY

Quantum phase transitions occur in the attractive Hubbard model at zero temperature as the external magnetic field and chemical potential are varied across any phase boundary in Fig. 2. In general, near a quantum critical point, the model is expected to show universal scaling behaviour in the thermodynamic quantities due to the collective nature of many-body effects⁶¹. We see that the 1D attractive Hubbard model is an ideal model to explore such a universal scale-invariant description on a 1D lattice, which can be determined by the power-law scaling of the various thermodynamic properties. The behavior of the thermodynamic quantities is governed

by scaling functions with critical exponents in the V-shaped region fanning out to finite temperatures from the quantum critical point. In order to calculate the thermodynamic quantities which contain enough thermal and quantum fluctuations to describe quantum criticality, we here use the form of the equation of state with the results given in (42), (43), and (45)-(47) for the pressure terms. We observe that first-order derivatives of these pressures with respect to μ or B form a set of linear equations. Solution to this set of linear equations directly leads to the particle density $n_c = \left(\frac{\partial p}{\partial \mu}\right)_B$ and magnetization $m = \frac{1}{2} \left(\frac{\partial p}{\partial B}\right)_\mu$. Similarly, one can derive the second-order derivatives of the pressures, the compressibility $\kappa = \left(\frac{\partial n}{\partial \mu}\right)_B$ and the susceptibility $\chi = \left(\frac{\partial m}{\partial B}\right)_\mu$. The corresponding scaling laws can be obtained in the different physical regimes.

At very low temperatures, spin fluctuation in the FFLO-like phase is suppressed, as are the bound states of higher k - Λ strings for $|\mu/T| \gg 1$. In this regime, the thermodynamics of the model is governed by a two-component TLL or say two-component Fermi liquid consisting of excess fermions and of hard-core bosonic charge bound states. The leading low-temperature correction to the free energy is given by

$$f \approx f_0 - \frac{\pi T^2}{6} \left(\frac{1}{v_1} + \frac{1}{v_2} \right), \quad (52)$$

where f_0 is the ground state free energy and v_1 (v_2) is the sound velocity of excess fermions (bound pairs). This result is valid for arbitrary interaction strength. When the particle density is very low, i.e., $n_{1,2} \ll 1$, we explicitly obtain the two velocities

$$\begin{aligned} v_1 &\approx 2\pi n_1 \left[1 + 4 \frac{n_2}{|u|} + 12 \left(\frac{n_2}{|u|} \right)^2 \right], \\ v_2 &\approx \pi n_2 \frac{\sqrt{2\alpha_1}}{\beta_1} \left[1 + \frac{1}{\beta_1} \left(2 \frac{n_1}{|u|} + \frac{n_2}{|u|} \right) \right. \\ &\quad \left. + \frac{3}{\beta_1^2} \left(2 \frac{n_1}{|u|} + \frac{n_2}{|u|} \right)^2 \right], \end{aligned} \quad (53)$$

where the lattice parameters

$$\begin{aligned} \alpha_1 &= \int_{-\pi}^{\pi} dk \frac{2|u| \cos^2 k (u^2 - 3 \sin^2 k)}{\pi (\sin^2 k + u^2)^3}, \\ \beta_1 &= \int_{-\pi}^{\pi} dk a_1(\sin k), \end{aligned} \quad (54)$$

are functions of $|u|$ representing the lattice effect⁶². In the above equations, $n_{1,2}$ stands for the densities of excess fermions and the bound pairs, respectively. We plot the two lattice parameters against interaction strength in Fig. 4. We shall see that the critical exponents and thermodynamics of the model are subject to these two parameters. The susceptibility is independent of temperature

so that the dimensionless Wilson ratio reaches a constant (we will study this nature of the Fermi liquid in the next section). The TLL validates only in the region below the crossover temperatures, where the entropy or specific heat retains a linear temperature-dependence, see the dashed lines in Fig. 5. The entropy in the temperature-magnetic field plane displays the visible areas of the critical regions (QC) near different critical points. In what follows, we will derive the scaling functions for the critical regions.

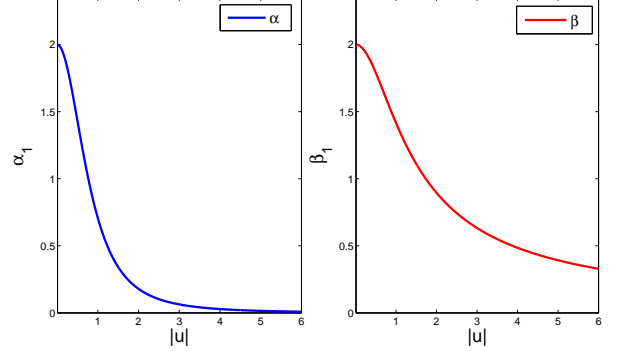


FIG. 4: The lattice interacting parameters for the length-1 $k - \Lambda$ strings as a function of the interaction strength u . The parameter α_1 strongly affects the band dispersion of bound pairs. The parameter β_1 presents a lattice contribution to the free energy of the pairs.

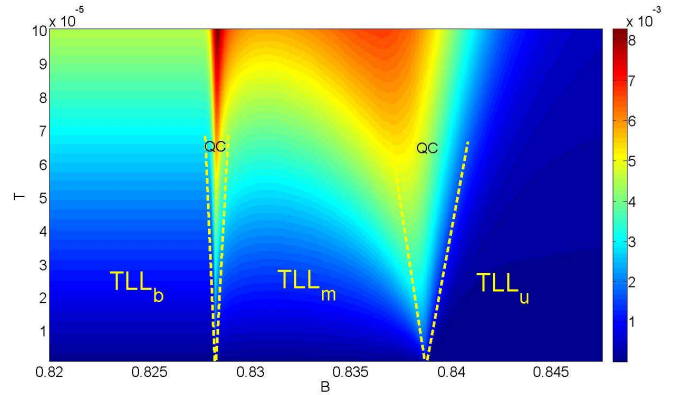


FIG. 5: Contour plot entropy vs. magnetic field B for the 1D attractive Hubbard model. The numerical calculation is performed by solving the TBA equations (17)-(19) with a fixed chemical potential $\mu = -0.828$ and interaction $u = -1$. The crossover temperatures (white dashed lines) fanning out from the critical points separate different TLL phases from the quantum critical regimes. The linear temperature-dependent entropy breaks down when the temperature is greater than these crossover temperatures. Here TLL_u and TLL_b respectively stand for the TLLs of unpaired fermions and bound pairs. TLL_m stands for the two-component TLL of the FFLO-like state.

Using the equation of state with the pressures (42),

(43), and (45)-(47), we can further derive the scaling forms of the thermodynamic quantities in the critical regimes. Analytic results for the scaling functions help to understand the microscopic origin of quantum criticality of the 1D attractive Hubbard model. For convenience, we first simplify the auxiliary functions

$$\begin{aligned}\delta &= \frac{1}{\pi} \int_{-1}^1 dx \frac{1}{1 + e^{2x/T}/\bar{z}_0} \frac{x}{\sqrt{1-x^2}}, \\ \gamma &= \frac{1}{\pi} \int_{-1}^1 dx \frac{1}{1 + e^{2x/T}/\bar{z}_0} \frac{1}{\sqrt{1-x^2}}, \\ \gamma' &= \frac{1}{\pi T} \int_{-1}^1 dx \frac{e^{2x/T}/\bar{z}_0}{(1 + e^{2x/T}/\bar{z}_0)^2} \frac{1}{\sqrt{1-x^2}}, \\ \delta' &= \frac{1}{\pi T} \int_{-1}^1 dx \frac{e^{2x/T}/\bar{z}_0}{(1 + e^{2x/T}/\bar{z}_0)^2} \frac{x}{\sqrt{1-x^2}},\end{aligned}\quad (55)$$

where $\bar{z}_0 = \exp\left(\mu + 2u + B + T^{\frac{3}{2}}g_{\frac{3}{2}}/\sqrt{\pi D_0}\right)$ with D_0 given in (51). By virtue of results (42), (43), and (45)-(47), the closed form expressions for thermodynamic quantities can be derived. For strong attraction, we have the relations

$$n_c = \gamma + (1 - \gamma) \frac{\partial p^b}{\partial \mu}, \quad (56)$$

$$m = \frac{1}{2} \left[\gamma + (1 - \gamma) \frac{\partial p^b}{\partial B} \right], \quad (57)$$

$$\kappa = \left(1 - \frac{\partial p^b}{\partial \mu}\right)^2 \gamma' + (1 - \gamma) \frac{\partial^2 p^b}{\partial \mu^2}, \quad (58)$$

$$\chi = \frac{1}{2} \left[\left(1 - \frac{\partial p^b}{\partial B}\right)^2 \gamma' + (1 - \gamma) \frac{\partial^2 p^b}{\partial B^2} \right], \quad (59)$$

for thermodynamic quantities. Here we calculated the derivatives of the pressures

$$\frac{\partial p^b}{\partial \mu} = -\frac{\tau^{\frac{1}{2}} \left(2f_{\frac{1}{2}} - \tau f_{\frac{3}{2}}\right)}{\Delta_t}, \quad (60)$$

$$\frac{\partial p^b}{\partial B} = -\frac{2\delta\tau^{\frac{1}{2}} \left(f_{\frac{1}{2}} - \tau f_{\frac{3}{2}}\right)}{|u|\Delta_t}, \quad (61)$$

$$\frac{\partial^2 p^b}{\partial \mu^2} = -\frac{f_{-\frac{1}{2}} \left(16\pi - \sqrt{\pi}\tau^{\frac{3}{2}}f_{\frac{3}{2}}\right)}{4D_0\tau^{\frac{1}{2}}\Delta_t^3}, \quad (62)$$

$$\begin{aligned}\frac{\partial^2 p^b}{\partial B^2} &= -\frac{2\delta'\tau^{\frac{1}{2}} \left(f_{\frac{1}{2}} - \tau f_{\frac{3}{2}}\right)}{|u|\Delta_t} - \frac{\pi\delta^2 f_{-\frac{1}{2}}}{u^2 D_1 \tau^{\frac{1}{2}} \left(4f_{\frac{1}{2}} - \tau f_{\frac{3}{2}}\right) \Delta_t^4} \\ &\quad \times \left(16\sqrt{\pi}f_{\frac{1}{2}} - 8\tau^{\frac{1}{2}}f_{\frac{3}{2}}^2 - 5\tau^{\frac{3}{2}}f_{\frac{1}{2}}f_{\frac{3}{2}} - 4\sqrt{\pi}\tau f_{\frac{3}{2}}\right)\end{aligned}\quad (63)$$

with $\tau = T/D_0$ and $\Delta_t = \sqrt{\pi} - \frac{1}{2}\tau^{\frac{1}{2}}f_{\frac{1}{2}} + \frac{1}{8}\tau^{\frac{3}{2}}f_{\frac{3}{2}}$. These results constitute very accurate results for the thermodynamics. The asymptotic results for the thermodynamic properties (56)-(59) have been demonstrated in Fig. 3.

The universality class of quantum criticality is determined by the critical exponents. As we have seen in

Fig. 2, the 1D attractive Hubbard model has a rich phase diagram. At least one branch of the density of states shows sudden change when the driving parameters vary across the phase boundary in the phase diagram. The singular behavior of thermodynamic properties is uniquely determined by the critical exponents, which are independent of the microscopic details of the system. Indeed, quantum criticality of quantum many-body systems depends solely on the dimensionality and the symmetry of the Hamiltonian. Here we expand the above equations of state for the thermodynamic quantities in the limit $|\mu - \mu_c| \ll T$. We derive the scaling forms of the thermodynamics at quantum criticality and thus read off the critical exponents.

We find that the suddenly changed density of state usually results in a quantum phase transition, so that the thermodynamical properties can be cast into the forms of universal quantum scaling functions in the critical region. For example, for the phase transition from the fully-paired phase V to the FFLO-like state IV, thermodynamic quantities of excess fermions display the singular parts in the scaling functions, whereas the thermodynamic properties of the bound pairs present the regular parts. In contrast to the attractive SU(2) Fermi gas, the half-filling phase in the attractive Hubbard model contributes a constant regular part to the thermodynamic quantities due to its unique band-filling.

Our results for the scaling functions of particle density, magnetization, compressibility and susceptibility are summarized as follows:

- phase transition (I-V),

$$\begin{aligned}n_c &= -\sqrt{\frac{2|u|}{\pi}} T^{\frac{1}{2}} \text{Li}_{\frac{1}{2}} \left(-\exp\left(\frac{2\mu - 2\mu_{c1}}{T}\right) \right), \\ m &\approx 0, \\ \kappa &= -2\sqrt{\frac{2|u|}{\pi}} T^{-\frac{1}{2}} \text{Li}_{-\frac{1}{2}} \left(-\exp\left(\frac{2\mu - 2\mu_{c1}}{T}\right) \right), \\ \chi &\approx 0.\end{aligned}\quad (64)$$

- phase transition (I-II),

$$\begin{aligned}n_c &= -\frac{1}{2\sqrt{\pi}} T^{\frac{1}{2}} \text{Li}_{\frac{1}{2}} \left(-\exp\left(\frac{\mu - \mu_{c2}}{T}\right) \right), \\ m &= -\frac{1}{4\sqrt{\pi}} T^{\frac{1}{2}} \text{Li}_{\frac{1}{2}} \left(-\exp\left(\frac{\mu - \mu_{c2}}{T}\right) \right), \\ \kappa &= -\frac{1}{2\sqrt{\pi}} T^{-\frac{1}{2}} \text{Li}_{-\frac{1}{2}} \left(-\exp\left(\frac{\mu - \mu_{c2}}{T}\right) \right), \\ \chi &= -\frac{1}{4\sqrt{\pi}} T^{-\frac{1}{2}} \text{Li}_{-\frac{1}{2}} \left(-\exp\left(\frac{\mu - \mu_{c2}}{T}\right) \right).\end{aligned}\quad (65)$$

- phase transition (II-III),

$$\begin{aligned}n_c &= 1 + \frac{1}{2\sqrt{\pi}} T^{\frac{1}{2}} \text{Li}_{\frac{1}{2}} \left(-\exp\left(-\frac{\mu - \mu_{c3}}{T}\right) \right), \\ m &= \frac{1}{2} + \frac{1}{4\sqrt{\pi}} T^{\frac{1}{2}} \text{Li}_{\frac{1}{2}} \left(-\exp\left(-\frac{\mu - \mu_{c3}}{T}\right) \right),\end{aligned}$$

$$\begin{aligned}\kappa &= -\frac{1}{2\sqrt{\pi}} T^{-\frac{1}{2}} \text{Li}_{-\frac{1}{2}} \left(-\exp \left(-\frac{\mu - \mu_{c3}}{T} \right) \right), \\ \chi &= -\frac{1}{4\sqrt{\pi}} T^{-\frac{1}{2}} \text{Li}_{-\frac{1}{2}} \left(-\exp \left(-\frac{\mu - \mu_{c3}}{T} \right) \right).\end{aligned}\quad (66)$$

- phase transition (II-IV),

$$\begin{aligned}n_c &= n_{b4} + \lambda_1 T^{\frac{1}{2}} \text{Li}_{\frac{1}{2}} \left(-\exp \left(\frac{2(\mu - \mu_{c4})}{T} \right) \right), \\ m &= m_{b4} + \lambda_2 T^{\frac{1}{2}} \text{Li}_{\frac{1}{2}} \left(-\exp \left(\frac{2(\mu - \mu_{c4})}{T} \right) \right), \\ \kappa &= \kappa_{b4} + \lambda_3 T^{-\frac{1}{2}} \text{Li}_{-\frac{1}{2}} \left(-\exp \left(\frac{2(\mu - \mu_{c4})}{T} \right) \right), \\ \chi &= \chi_{b4} + \lambda_4 T^{-\frac{1}{2}} \text{Li}_{-\frac{1}{2}} \left(-\exp \left(\frac{2(\mu - \mu_{c4})}{T} \right) \right).\end{aligned}\quad (67)$$

- phase transition (V-IV),

$$\begin{aligned}n_c &= n_{b5} + \lambda_5 T^{1/2} \text{Li}_{1/2} \left(-\exp \left(\frac{\mu - \mu_{c5}}{T} \right) \right), \\ m &= -\frac{1}{4\sqrt{\pi}} T^{1/2} \text{Li}_{1/2} \left(-\exp \left(\frac{\mu - \mu_{c5}}{T} \right) \right), \\ \kappa &= \kappa_{b5} + \lambda_6 T^{-1/2} \text{Li}_{-1/2} \left(-\exp \left(\frac{\mu - \mu_{c5}}{T} \right) \right), \\ \chi &= -\frac{1}{4\sqrt{\pi}} T^{-1/2} \text{Li}_{-1/2} \left(-\exp \left(\frac{\mu - \mu_{c5}}{T} \right) \right).\end{aligned}\quad (68)$$

In the above scaling forms some constants are given in Appendix VII C. These scaling forms can be cast into the form of well known universal scaling laws. For example, the universal scaling laws for the density and compressibility read^{61,63–65}

$$\begin{aligned}n(\mu, B, T) &= n_0(\mu, B, T) + T^{d/z+1-(1/\nu z)} \mathcal{G} \left(\frac{\mu - \mu_c}{T^{1/\nu z}} \right), \\ \kappa(\mu, B, T) &= \kappa_0(\mu, B, T) + T^{d/z+1-(2/\nu z)} \mathcal{F} \left(\frac{\mu - \mu_c}{T^{1/\nu z}} \right),\end{aligned}\quad (69)$$

where n_0 and κ_0 are the regular parts, i.e., the background values before the phase transition. Meanwhile $\mathcal{G}(x) = \text{Li}_{\frac{1}{2}}(x)$, $\mathcal{F}(x) = \text{Li}_{-\frac{1}{2}}(x)$ give the scaling functions in the singular parts. From the above scaling forms, we read off the dynamical exponent $z = 2$ and correlation critical exponent $\nu = 1/2$. This scaling theory is valid for all phase transitions across the phase boundaries in the phase diagram 2. Such universal scaling laws are demonstrated in Fig. 6 for various phase transitions.

The above scaling forms are observed to give the same critical exponents which characterize the universality class of free-fermion criticality. An intuitive explanation for this result is that the phase transitions occurred in the 1D Hubbard model have a common feature: at least one branch of Fermi sea vanishing, namely $\varepsilon^{u,b}(0) = 0$. This naturally leads to a change in dispersion, i.e., a linear

dispersion vanishes while a quadratic dispersion is created when the phase transition occurs. This change in dispersion underlies a universality class of quantum criticality, see also the recent studies of the 1D interacting Bose gas⁶⁶ and the 1D Heisenberg spin chain⁶⁷.

Moreover, the phase V in the phase diagram Fig. 2 shows a gapped phase (fully paired phase), where the susceptibility reveals a particular exponential decay at low temperatures. Using the equation of state with the pressures (42), (43), and (45)-(47), we further show that the susceptibility decays exponentially with the energy gap induced by the ferromagnetic ordering, namely

$$\chi \approx \frac{T^{-1/2}}{4\sqrt{\pi}} e^{-\Delta/T}, \quad (70)$$

where the energy gap is given by $\Delta = \varepsilon^u(0) = -2 - \mu - 2u - B + p^b$ with $p^b = \frac{4(2\pi - q^3/3)}{3|u|\pi} \left(1 + \frac{2|u|\pi\mu}{2\pi - q^3/3} \right)^{\frac{3}{2}}$. This result can also be obtained by applying Sommerfeld expansion in Eq. (48). We approximately obtain the susceptibility $\chi \approx \frac{1}{2}\gamma' \approx -\frac{T^{-1/2}}{2\sqrt{\pi}} \text{Li}_{-\frac{1}{2}}(-e^{-\Delta/T})$ from Eq. (59). In the next section, we further demonstrate the macroscopic nature of the susceptibility in the FFLO phase.

V. FREE FLUIDS AND ADDITIVITY RULES

Fermi liquid theory is believed to break down in 1D strongly correlated systems due to the absence of well defined quasi-particles⁵⁸. Consequently the TLL theory is generally believed to describe the collective low-lying excitations in 1D many-body systems. Despite such a big difference in the microscopic origins of the two low-energy theories, both the Fermi liquid and the TLL share a common feature – a small distortion of the Fermi surface or Fermi points results in the universal low-energy physics of many-body systems. From the results of the last section, we observed that at very low temperatures the low-energy physics of the FFLO-like state is governed by the universality class of a two-component TLL. However, in view of the macroscopic properties of the 1D attractive Hubbard model, we argue that such a universality class of two-component TLL reveals an important nature of free fluids. In order to show this elegant nature, we will introduce two effective chemical potentials for the excess fermions and bound pairs on a 1D lattice. Then we will show that the thermodynamic properties in the FFLO-like phase behave like two independent free fluids. In particular, we find simple additivity rules for the compressibility and susceptibility which represent a universal characteristic of quantum liquids at the renormalization fixed point.

Prior to a discussion of the free fluids, we first make an approximation for the zero temperature TBA equations Eqs. (21) and (22) in the low density regime,

$$\varepsilon^1(k) = k^2 - \mu_1 - a_1 \star \varepsilon^2(k), \quad (71)$$

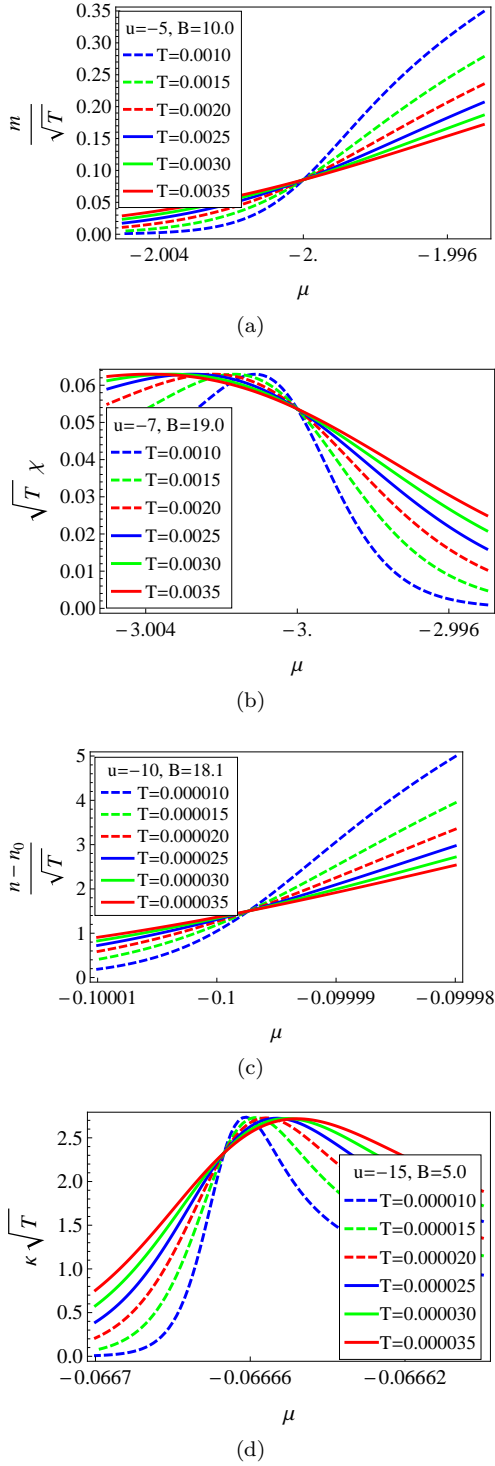


FIG. 6: Scaling laws for thermodynamic quantities vs. chemical potential at different temperatures. The intersection points in (a), (b), (c) and (d) give the critical points for phase transitions (I-II), (II-III), (II-IV) and (I-V), respectively.

$$\varepsilon^2(\Lambda) = \alpha_1 \Lambda^2 - \alpha_1 \mu_2 - a_1 \star \varepsilon^1(\Lambda) - a_2 \star \varepsilon^2(\Lambda), \quad (72)$$

where $a_m \star \varepsilon^n(x) = \int_{-y_c}^{y_c} dy a_m(x-y) \varepsilon^n(y)$ with y_c being the Fermi point of $\varepsilon^n(y)$, i.e., $\varepsilon^n(y_c) = 0$. In the above

equations, we introduced the effective chemical potentials for excess fermions and bound pairs as

$$\mu_1 = \mu + B + 2u + 2, \quad (73)$$

$$\mu_2 = \frac{2}{\alpha_1} \left(\mu + 2\sqrt{u^2 + 1} - 2|u| \right). \quad (74)$$

The effective chemical potential of the bound pairs reveals a deep physical insight into the crossover from Bose-Einstein condensate (BEC) to Bardeen-Cooper-Schrieffer (BCS) superconductor. Later we shall see these effective chemical potentials reveal an important free quantum liquid nature. We will show that for the balanced case the effective chemical potential μ_2 varies from the kinetic energy of bound pairs to the free Fermi energy when the interaction changes from negative infinity to zero. This reveals a 1D analogue of the BEC-BCS crossover. This form of the TBA equations is useful to access the ground state properties, such as sound velocities, stiffness and effective chemical potentials. By virtue of Eqs. (71) and (72) we rewrite the free energy per site (20) as

$$f = u + \int_{-k_c}^{k_c} \frac{dk}{2\pi} \varepsilon^1(k) + \int_{-\Lambda_c}^{\Lambda_c} \frac{d\Lambda}{2\pi} \beta_1 \varepsilon^2(\Lambda), \quad (75)$$

where $\varepsilon^u = \varepsilon^1$ and $\varepsilon'_1 = \varepsilon^2$.

We now proceed to calculate the TLL parameters of the model and compare them with those of the 1D attractive SU(2) Fermi gas⁶⁰. The basic idea is to express the effective chemical potentials in terms of the Fermi points by employing iteration of Eqs. (71) and (72). Using the fact that the two dressed energies vanish at their corresponding Fermi points, we express those Fermi points in terms of the densities of excess fermions and bound pairs. We shall see that this process leads to a separation of two free fluids in the ground state energy per site.

In order to simplify the lengthy iterations, we firstly rescale the TBA equations (71) and (72) by defining $\tilde{\varepsilon}^n = \varepsilon^n/u^2$, $\tilde{\mu}_n = \mu_n/u^2$, $\tilde{y}_c = y_c/|u|$, and $\tilde{a}_n(x) = \frac{n}{\pi} \frac{1}{n^2+x^2}$. Then we introduce a vector presentation of the rescaled TBA equations. In view of the properties of even functions, we utilize the base $\{k^{2n}\}$ and $\{\Lambda^{2n}\}$ ($n = 0, 1, 2, \dots$) to expand these scalar equations, thus we have, respectively

$$\vec{\varepsilon}^1 = \vec{V}^1 - \mathbf{A}^1(\tilde{\Lambda}_c) \vec{\varepsilon}^2, \quad (76)$$

$$\vec{\varepsilon}^2 = \vec{V}^2 - \mathbf{A}^1(\tilde{k}_c) \vec{\varepsilon}^1 - \mathbf{A}^2(\tilde{\Lambda}_c) \vec{\varepsilon}^2. \quad (77)$$

The vectors $\vec{V}^1 = [-\tilde{\mu}_1, 1, 0, \dots]^t$ and $\vec{V}^2 = [-\alpha_1 \tilde{\mu}_2, \alpha_1, 0, \dots]^t$ are the driving terms and the superscript t represents transpose operation. The matrix $\mathbf{A}^n(\tilde{y}_c) \vec{\varepsilon}$ corresponds to the integral $\int_{-\tilde{y}_c}^{\tilde{y}_c} dy \tilde{a}_n(x-y) \vec{\varepsilon}(y)$.

Furthermore, as we only retain the first few leading terms, $\vec{\varepsilon}^n$ and $\mathbf{A}^n(\tilde{y}_c)$ can be expanded as sums of a few leading orders with respect to y_c , i.e., $\vec{\varepsilon}^n = \vec{\varepsilon}_{(0)}^n + \vec{\varepsilon}_{(1)}^n + \vec{\varepsilon}_{(2)}^n + \dots$ and $\mathbf{A}^n(\tilde{y}_c) = \mathbf{A}_{(1)}^n(\tilde{y}_c) + \mathbf{A}_{(3)}^n(\tilde{y}_c) + \mathbf{A}_{(5)}^n(\tilde{y}_c) + \dots$. More details of the latter expansion are presented

in section VII D. Substituting these expansions into the TBA equations of vectorial form Eqs. (76) and (77), and sorting terms order by order, leads to the set of equations

$$\begin{aligned}
\bar{\varepsilon}_{(0)}^1 &= \bar{V}^1, & \bar{\varepsilon}_{(0)}^2 &= \bar{V}^2, \\
\bar{\varepsilon}_{(1)}^1 &= -\mathbf{A}_{(1)}^1(\tilde{\Lambda}_c)\bar{\varepsilon}_{(0)}^2, \\
\bar{\varepsilon}_{(1)}^2 &= -\mathbf{A}_{(1)}^1(\tilde{k}_c)\bar{\varepsilon}_{(0)}^1 - \mathbf{A}_{(1)}^2(\tilde{\Lambda}_c)\bar{\varepsilon}_{(0)}^2, \\
\bar{\varepsilon}_{(2)}^1 &= -\mathbf{A}_{(1)}^1(\tilde{\Lambda}_c)\bar{\varepsilon}_{(1)}^2, \\
\bar{\varepsilon}_{(2)}^2 &= -\mathbf{A}_{(1)}^1(\tilde{k}_c)\bar{\varepsilon}_{(1)}^1 - \mathbf{A}_{(1)}^2(\tilde{\Lambda}_c)\bar{\varepsilon}_{(1)}^2, \\
\bar{\varepsilon}_{(3)}^1 &= -\mathbf{A}_{(1)}^1(\tilde{\Lambda}_c)\bar{\varepsilon}_{(2)}^2 - \mathbf{A}_{(3)}^1(\tilde{\Lambda}_c)\bar{\varepsilon}_{(0)}^2, \\
\bar{\varepsilon}_{(3)}^2 &= -\mathbf{A}_{(1)}^1(\tilde{k}_c)\bar{\varepsilon}_{(2)}^1 - \mathbf{A}_{(1)}^2(\tilde{\Lambda}_c)\bar{\varepsilon}_{(2)}^2 - \mathbf{A}_{(3)}^1(\tilde{k}_c)\bar{\varepsilon}_{(0)}^1 \\
&\quad - \mathbf{A}_{(3)}^2(\tilde{\Lambda}_c)\bar{\varepsilon}_{(0)}^2.
\end{aligned} \tag{78}$$

It is easy to solve the above vectorial forms $\bar{\varepsilon}_{(r)}^1$ and $\bar{\varepsilon}_{(r)}^2$ with $r = 1, 2, 3$. We then substitute these results into the scalar expression of the rescaled TBA equations. Together with $\bar{\varepsilon}^n(\tilde{y}_c) = 0$ and the expansion $\tilde{\mu}_n = \tilde{\mu}_n^{(2)} + \tilde{\mu}_n^{(3)} + \tilde{\mu}_n^{(4)} + \dots$, we then obtain a set of recurrence equations for $\tilde{\mu}_n^{(2)}$, $\tilde{\mu}_n^{(3)}$ and $\tilde{\mu}_n^{(4)}$. Here we observe that the expansions for chemical potentials begin from $n = 2$ due to the fact that $\bar{\varepsilon}^1(\tilde{k}_c) = -\tilde{\mu}_1 + \tilde{k}_c^2 + o(\tilde{k}_c^3) = 0$, i.e., $\tilde{\mu}_1 = \tilde{k}_c^2 + o(\tilde{k}_c^3)$. Similarly for $\tilde{\mu}_2$. We solve these equations and then express the solution as the vectorial equation

$$\begin{bmatrix} \tilde{\mu}_1 \\ \alpha_1 \tilde{\mu}_2 \end{bmatrix} = \left(\mathbf{I} + \frac{2}{3} \mathbf{T} \right) \begin{bmatrix} \tilde{k}_c^2 \\ \alpha_1 \tilde{\Lambda}_c^2 \end{bmatrix}, \tag{79}$$

where the matrix \mathbf{T} is given by

$$\mathbf{T} = \frac{1}{\pi} \begin{bmatrix} 0 & 2\tilde{\Lambda}_c \\ 2\tilde{k}_c & \tilde{\Lambda}_c \end{bmatrix}. \tag{80}$$

Finally, the free energy per site Eq. (75) is expressed in terms of Fermi points k_c and Λ_c , with result

$$f = -\frac{2}{3\pi} (k_c^3 + \alpha_1 \beta_1 \Lambda_c^3) + u. \tag{81}$$

We now proceed to obtain the particle densities in terms of the Fermi points. To this end, we turn to the total particle density n_c and magnetization \bar{m} per site based on Eq. (75),

$$\begin{aligned}
n_c &= -\frac{\partial f}{\partial \mu} = -\int_{-k_c}^{k_c} \frac{dk}{2\pi} \frac{\partial \varepsilon^1}{\partial \mu} - \beta_1 \int_{-\Lambda_c}^{\Lambda_c} \frac{d\Lambda}{2\pi} \frac{\partial \varepsilon^2}{\partial \mu}, \\
\bar{m} &= -\frac{\partial f}{\partial B} = -\int_{-k_c}^{k_c} \frac{dk}{2\pi} \frac{\partial \varepsilon^1}{\partial B} - \beta_1 \int_{-\Lambda_c}^{\Lambda_c} \frac{d\Lambda}{2\pi} \frac{\partial \varepsilon^2}{\partial B}.
\end{aligned}$$

In order to get closed forms for these two properties, we first take partial derivatives of Eqs. (71) and (72) with respect to μ and B , respectively. Then we rewrite these integral equations in terms of the vectorial forms similar

to Eqs. (76) and (77). Finally, by lengthy iteration and after some manipulations, we obtain

$$\begin{bmatrix} \tilde{n}_1 \\ \tilde{n}_2 \end{bmatrix} = \frac{1}{\pi} (\mathbf{I} - \mathbf{T} + \mathbf{T}^2)^t \begin{bmatrix} \tilde{k}_c \\ \beta_1 \tilde{\Lambda}_c \end{bmatrix}, \tag{82}$$

where $\tilde{n}_r = n_r/|u|$ ($r = 1, 2$) with $n_1 = \bar{m}$ and $n_2 = (n_c - n_1)/2$ being respectively the densities for the excess fermions and bound pairs. Here the redefined $\bar{m} = 2m$ is introduced according to the original TBA equations. An inverse of Eq. (82) gives the cut-off momenta in terms of the densities $n_{1,2}$

$$\begin{aligned}
k_c &\approx \pi n_1 \sum_{n=0}^3 \left(\frac{2n_2}{|u|} \right)^n, \\
\Lambda_c &\approx \frac{\pi n_2}{\beta_1} \sum_{n=0}^3 \left[\frac{2n_1 + n_2}{\beta_1 |u|} \right]^n.
\end{aligned} \tag{83}$$

For the next step, substituting Eq. (83) into (81), leads to separating the ground state energy per site into the energies of excess fermions and bound pairs, with result

$$e = e_1 + e_2 + e_b. \tag{84}$$

Here e_b is the binding energy and the subscripts 1 and 2 denote the excess fermions and bound pairs, respectively. The terms are given explicitly by

$$\begin{aligned}
e_1 &= \frac{\pi^2}{3} n_1^3 \left[1 + 2 \left(\frac{2n_2}{|u|} \right) + 3 \left(\frac{2n_2}{|u|} \right)^2 \right], \\
e_2 &= \frac{\pi^2}{3} \frac{\alpha_1 n_2^3}{\beta_1^2} \left[1 + 2 \left(\frac{2n_1 + n_2}{\beta_1 |u|} \right) + 3 \left(\frac{2n_1 + n_2}{\beta_1 |u|} \right)^2 \right],
\end{aligned} \tag{85}$$

$$e_b = -(2u + 2)n_1 - 4 \left(u + \sqrt{u^2 + 1} \right) n_2. \tag{86}$$

As usual, we define a dimensionless interaction strength $\gamma_s = 2|u|/n_s$ ($s = 1, 2$)⁶⁰. Using the relation

$$K_s = \pi / \sqrt{3e(\gamma_s) - 2\gamma_s \frac{de(\gamma_s)}{d\gamma_s} + \frac{1}{2}\gamma_s^2 \frac{d^2e(\gamma_s)}{d\gamma_s^2}}, \tag{87}$$

the Luttinger parameters for the excess fermions and bound pairs can be directly worked out to be

$$K_1 = 1, \quad K_2 = 2\sqrt{2} \frac{\beta_1}{\sqrt{\alpha_1}} \left[1 - \frac{2}{\beta_1 \gamma_2} + \frac{1}{(\beta_1 \gamma_2)^2} \right]. \tag{88}$$

We note that the Luttinger parameter K_2 in the fully paired phase depends explicitly on the lattice parameters α_1 and β_1 . This behavior is different from the constant value $K_2 = 4$ for the bound pairs phase of the strongly attractive SU(2) Fermi gas⁶⁰. In the limits $u \rightarrow 0$ and $n_s/|u|$ small, the lattice parameters $\alpha_1 \rightarrow 2$, $\beta_1 \rightarrow 2$. Thus we have $K_2 = 4$ which is the same as for the SU(2) Fermi gas. The two limits $u \rightarrow 0$ and $n_s/|u| \ll 1$ represent the lattice-gas mapping between 1D attractive Hubbard model and SU(2) Fermi gas⁹.

Beside this framework of the TLL theory, we also find that for the low density case, the chemical potentials for the unpaired fermions and pairs are given explicitly by

$$\mu_1 = \pi n_1^2 A_1^2 + \frac{4\pi^2 \alpha_1}{3\beta_1^3 |u|} n_2^3 A_2^3, \quad (90)$$

$$\mu_2 = \pi^2 \frac{n_2^2}{\beta_1^2} A_2^2 + \frac{4\pi^2}{3\alpha_1 |u|} n_1^3 A_1^3 + \frac{2\pi^2}{3\beta_1^3 |u|} n_2^3 A_2^3, \quad (91)$$

where $A_1 = 1 + \frac{2n_2}{|u|} + \left(\frac{2n_2}{|u|}\right)^2$ and $A_2 = 1 + \frac{2n_1+n_2}{\beta_1 |u|} + \left(\frac{2n_1+n_2}{\beta_1 |u|}\right)^2$, which indicate interacting effects among pairs and unpaired fermions. We observe that the chemical potential μ_2 tends to the kinetic energy of bound pairs in the BEC limit $|u| \rightarrow \infty$. Whereas in the weak coupling limit, $|u| \rightarrow 0$, μ_2 tends to the Fermi energy of the free fermions on a 1D lattice. The effective chemical potentials (90) and (91) reveal that the thermodynamic quantities could be separable, i.e., the total is equal to a sum of the effective thermodynamic quantities of two individual constituents.

Here we further derive the additivity rules for the compressibility and susceptibility. For the compressibility, using the standard thermodynamic relation $\kappa = \left(\frac{\partial n_c}{\partial \mu}\right)_B$, the derivatives of the density and effective chemical potentials for fixed magnetic field could be further expressed as $dn_c = dn_1 + 2dn_2$ and $d\mu_1 = \frac{\alpha_1}{2}d\mu_2 = d\mu$, respectively. Inserting these relations into the definition of compressibility, $\kappa = \frac{\partial n_c}{\partial \mu} \Big|_B = \frac{dn_1 + 2dn_2}{d\mu}$, we thus obtain

$$\kappa = \kappa_1 + \frac{2}{\alpha_1} \kappa_2. \quad (92)$$

Here the effective compressibilities of excess fermions and bound pairs are defined as $\kappa_1 = \left(\frac{\partial n_1}{\partial \mu_1}\right)_B$ and $\kappa_2 = 2\left(\frac{\partial n_2}{\partial \mu_2}\right)_B$. Details are given in see in Appendix VIII D. The additivity rule (92) for the compressibility can be confirmed numerically, as shown in Fig. 7(a).

For the susceptibility in the canonical ensemble, defined as $\bar{\chi} = \left(\frac{\partial \bar{n}}{\partial B}\right)_{n_c}$, it is straightforward to see $dn_c = dn_1 + 2dn_2 = 0$ and $dB = d\mu_1 - \frac{\alpha_1}{2}d\mu_2$, and thus the additivity rule

$$\frac{1}{\bar{\chi}} = \frac{1}{\bar{\chi}_1} + \frac{\alpha_1}{2} \frac{1}{\bar{\chi}_2}. \quad (93)$$

Here $\bar{\chi}_1 = \left(\frac{\partial n_1}{\partial \mu_1}\right)_{n_c}$ and $\bar{\chi}_2 = 2\left(\frac{\partial n_2}{\partial \mu_2}\right)_{n_c}$ are the effective susceptibilities for excess fermions and bound pairs, respectively. These explicit expressions for the effective thermodynamic quantities can be found in Appendix VIII D. The additivity rule (93) for the susceptibility can also be confirmed numerically, as shown in Fig. 7(b). Similar to the observation concerning TLL parameters, the additivity rules for the 1D attractive Hubbard model also reduce to those for the SU(2) Fermi gas through the

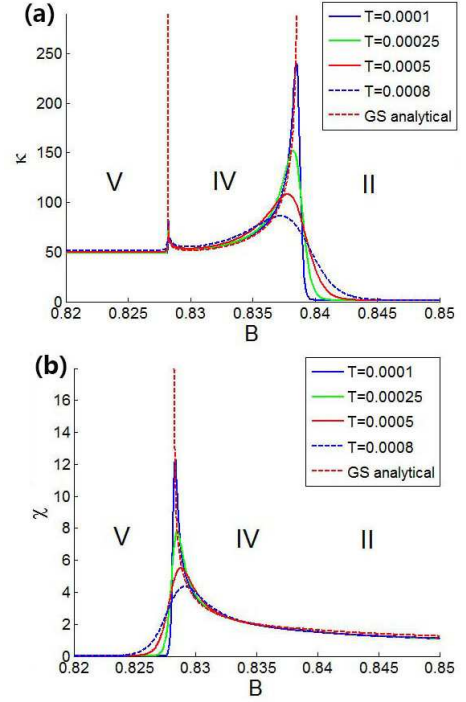


FIG. 7: Additivity rules: (a) Compressibility κ and (b) spin susceptibility χ vs. magnetic field B for the attractive Hubbard model with $u = -1$ and $\mu = -0.8282$. The red dashed lines show the result obtained from the additivity rules (92) and (93). At low temperatures, all compressibility and susceptibility curves collapse into the zero temperature ones obeying the additivity rules. In the vicinity of the critical points such free fluids nature breaks down.

lattice-gas mapping. In Appendix VIII D we calculate the individual compressibility and susceptibility explicitly.

The simple additivity nature of the thermodynamics at low temperatures characterizes the universal low energy physics of the FFLO-like state of the 1D attractive Hubbard model. In this sense, the additivity rules reflect a universal nature of the multicomponent TLL in 1D. The simple additivity rule thus reveals the significant two free fluid nature of the FFLO phase, as predicted in expansion dynamics of the FFLO state in 1D⁴⁴. The macroscopic magnetic properties in the FFLO-like phase show the properties of the ordinary higher-dimensional Fermi liquid, see Fig. 8. This figure shows that in the free fluids region the magnetization is nearly temperature independent. In the non-Fermi liquid region thermal fluctuations gradually overwhelm quantum fluctuations. Thus the magnetization has a uniform temperature dependence for different magnetic fields, indicating paramagnetism. The non-Fermi liquid crossover region reveals a scaling invariance, which was studied in Section IV. Such Fermi liquid-like features have been found in the spin compound $\text{Cu}(\text{C}_4\text{H}_4\text{N}_2)(\text{NO}_3)_2$ ⁵³ and the heavy fermion material YbNi_4P_2 ⁵⁴. The study of Fermi and non-Fermi liquids in 1D has received significant recent

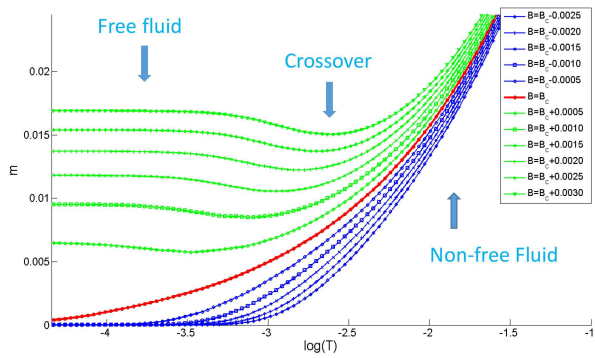


FIG. 8: Numerical results for the magnetization vs. logarithm of the temperature for different magnetic fields. Here we have set a fixed chemical potential $\mu = -0.14$ and interaction strength $u = -7$. For magnetic field $B > B_c = 12.11065$ (phase IV), three regions are clearly displayed: The free fluids region at low temperatures, non-Fermi liquid region at higher temperatures, and a crossover in between. For magnetic field $B < B_c$ (phase V), the magnetization displays the gapped nature of a non-Fermi liquid phase.

interest^{56,68,69}.

Using the explicit expressions for the compressibility (92) and susceptibility (93), we may calculate the Wilson ratio, which is a dimensionless ratio defined as the susceptibility or compressibility over the specific heat divided by the temperature. The Wilson ratio is the ratio describing quantum fluctuations and energy thermal fluctuations. Both the Fermi liquid and TLL give a constant Wilson ratio⁶⁰, i.e., two types of fluctuations are on equal-footing in temperature scaling. However, near a critical point, the dimensionless Wilson ratios exhibits a sudden enhancement indicating a sudden change in the density of state. Therefore the Wilson ratios serves as a powerful tool for distinguishing the phases of a quantum liquid and for determining the finite temperature phase diagram as well.

The compressibility Wilson ratio R_W is determined by

$$\begin{aligned} R_W^\kappa &= \frac{\pi^2 k_B^2}{3} \frac{\kappa}{C_v/T} \\ &= \pi \left(\kappa_1 + \frac{2}{\alpha_1} \kappa_2 \right) / \left(\frac{1}{v_1} + \frac{1}{v_2} \right), \end{aligned} \quad (94)$$

where we have used Eq. (52) to calculate the specific heat and set the Boltzmann constant to $k_B = 1$. This Wilson ratio vanishes in both phases I (vacuum) and III (half-filling phase). In the limit $n_c/|u| \rightarrow 0$ the compressibility Wilson ratio for phases II and IV are respectively, $R_W^\kappa = 1$ and $R_W^\kappa = 2\sqrt{2}\beta_1/\sqrt{\alpha_1}$. These results turn out to be the same as for the strongly attractive SU(2) Fermi gas⁶⁰ when the limit $u \rightarrow 0$ is applied. On the other hand, the susceptibility Wilson ratio is defined by $R_W^\chi = \frac{4}{3} \left(\frac{\pi k_B}{\mu_B g_L} \right)^2 \frac{\chi}{C_v/T}$ with Bohr magneton μ_B and Lande factor g_L . Fig. 9 shows a contour plot of each type

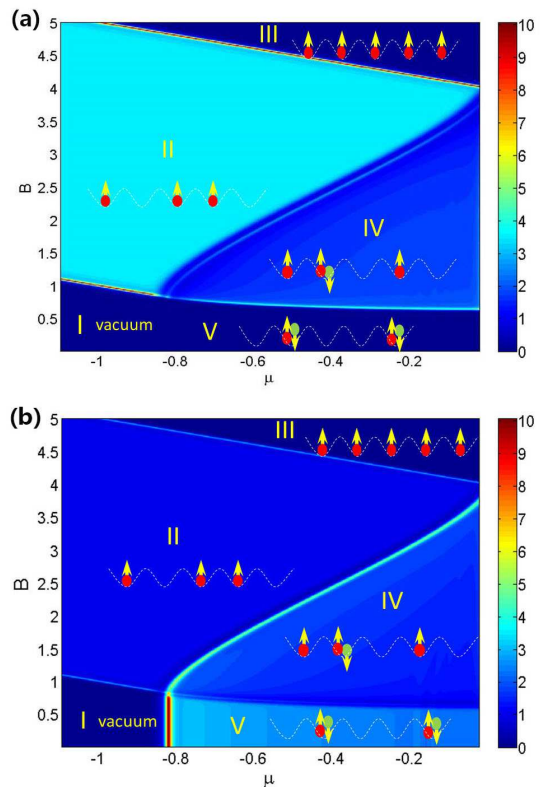


FIG. 9: Finite temperature phase diagrams obtained from contour plots of the Wilson ratios. The plots in (a) and (b) are determined from the susceptibility Wilson ratio R_W^χ and from the compressibility Wilson ratio R_W^κ , respectively. Here $u = -1$ and $T = 0.001$. The red balls and green balls represent up spin and down spin respectively. Both diagrams agree well with the zero temperature phase diagram Fig. 2, despite the fact that the plot in (a) cannot distinguish phase I and V due to the vanishing susceptibility in these two phases.

of Wilson ratio which demonstrates the macroscopic feature of the Fermi liquid nature. This figure also presents the low-temperature phase diagram in the $B - \mu$ plane.

VI. CONCLUSION

In summary we have presented a framework to determine the nature of quantum criticality and quantum liquids in the 1D attractive Hubbard model. We have obtained the universal thermodynamics of the model by solving the TBA equations. In particular, we have analytically derived the equation of state at low temperatures, from which we have obtained effective chemical potentials of excess fermions and bound pairs, along with the density, compressibility, susceptibility and specific heat in terms of the chemical potential μ , magnetic field B , temperature T and interaction strength constant. At quantum criticality the scaling forms of these thermal and magnetic properties have been obtained. The dy-

namical exponent $z = 2$ and correlation critical exponent $\nu = 1/2$, indicating the universality class of criticality of free fermion theory.

Our results provide strong evidence for the existence of two free fluids of bound pairs and of unpaired fermions, which were noticed in the expansion dynamics of the FFLO state in 1D⁴⁴. Regarding the nature of the two fluids in the attractive Hubbard model, we have shown that in the low-density regime the interaction effect resulting from the paired and unpaired fermions can be absorbed into effective chemical potentials of two non-interacting ideal gases. Consequently, the additivity rules in the compressibility and susceptibility of the 1D attractive Hubbard model hold as long as the dimensionless Wilson ratio remains a constant. This behavior significantly reflects the free fluids nature in thermodynamic properties of the model. In this phase, the FFLO pair correlation function

$$\begin{aligned} G_p(x, t) &= \langle \Psi_{\uparrow}^{\dagger}(x, t) \Psi_{\downarrow}^{\dagger}(x, t) \Psi_{\uparrow}(0, 0) \Psi_{\downarrow}(0, 0) \rangle \\ &\approx A_{p,1} \frac{\cos(\pi(n_{\uparrow} - n_{\downarrow})x)}{|x + i v_1 t|^{2\theta_1} |x + i v_2 t|^{2\theta_2}} \\ &\quad + A_{p,2} \frac{\cos(\pi(n_{\uparrow} - 3n_{\downarrow})x)}{|x + i v_1 t|^{2\theta_3} |x + i v_2 t|^{2\theta_4}}, \end{aligned} \quad (95)$$

shows a typical spatial oscillation which is a characteristic of the FFLO state. In the above equation, the exponents $\theta_1 \approx 1/2$, $\theta_2 \approx 1/2 + \frac{n_2}{|u|\beta_1}$, $\theta_3 \approx \frac{1}{2} - \frac{4n_2}{|u|\beta_1}$ and $\theta_4 \approx \frac{5}{2} - \frac{4n_1}{|u|} - \frac{3n_2}{|u|\beta_1}$ depend essentially on the lattice parameter β_1 . Here $n_{2,1} = N_{2,1}/L$ are the dimensionless densities of pairs and unpaired fermions, with the sound velocities $v_{1,2}$ given in (53). The study of the FFLO pair correlation is presented elsewhere³⁵. To conclude, we note that our work provides benchmark physics of the 1D attractive Hubbard model of relevance to experiments with ultracold fermionic atoms on lattices.

Acknowledgments. The authors SC and YCY contributed equally to the calculations in this paper.

The authors thank R. Hulet for helpful discussion. This work is supported by Key NNSFC grant number 11534014, MOST grant number 2017YFA0304500, NNSFC grant numbers 11374331, 11174375 and ARC Discovery Projects DP130102839, DP170104934.

VII. APPENDICES

A. Wiener-Hopf method

The phase boundary between phases IV and V is determined by the conditions $\varepsilon^u(0) = 0$ and $\varepsilon^b(0) < 0$, which imply that $Q = 0$ and A is finite. Thus at zero temperature the TBA equations are simplified to

$$\begin{aligned} \varepsilon^u(k) &= -2 \cos k - \mu - 2u - B \\ &\quad - \int_{-A}^A d\Lambda a_1(\sin k - \Lambda) \varepsilon'_1(\Lambda), \end{aligned} \quad (A1)$$

$$\begin{aligned} \varepsilon'_1(\Lambda) &= -2\mu - 2 \int_{-\pi}^{\pi} dk \cos^2 k a_1(\sin k - \Lambda) \\ &\quad - \int_{-A}^A d\Lambda' a_2(\Lambda - \Lambda') \varepsilon'_1(\Lambda'). \end{aligned} \quad (A2)$$

Particularly, if $A = \infty$, it follows that the chemical potential $\mu = 0$. The intersection of the phase boundary with the B -axis could be calculated exactly by the Fourier transformation

$$B_{c1} = 2|u| - 2 + 2 \int_0^{\infty} d\omega \frac{J_1(\omega) \exp(-|u|\omega)}{w \cosh(u\omega)}. \quad (A3)$$

Now we consider the more general case $A \gg 1$, for which the phase boundary can be resolved using the Wiener-Hopf method. By applying Fourier transformation on Eq. (A2) and after some algebraic manipulations, we have

$$\varepsilon'_1(\Lambda) = -\mu - \int_{-\infty}^{\infty} d\omega \frac{J_1(\omega)}{\omega \cosh(u\omega)} \exp(i\omega\Lambda) + \int_0^{\infty} d\Lambda' \varepsilon'_1(\Lambda' + A) [R(\Lambda - \Lambda' - A) + R(\Lambda + \Lambda' + A)], \quad (A4)$$

where we have introduced the function

$$R(x) = \int_{-\infty}^{\infty} \frac{d\omega}{2\pi} \frac{\exp(i\omega x)}{1 + \exp(2|u\omega|)}. \quad (A5)$$

Substituting $y(\Lambda) = \varepsilon'_1(\Lambda + A)$ and expanding $y(\Lambda) = \sum_{n=0}^{\infty} y_n(\Lambda)$ in terms of powers of Λ in Eq. (A4), the result can be separated into a series of Wiener-Hopf integral equations in terms of the functions $y_n(\Lambda)$, namely

$$y_n(\Lambda) = g_n(\Lambda) + \int_0^{\infty} d\Lambda' R(\Lambda - \Lambda') y_n(\Lambda'). \quad (A6)$$

Here we denote the driving terms

$$\begin{aligned} g_0(\Lambda) &= -\mu - \int_{-\infty}^{\infty} d\omega \frac{J_1(\omega) e^{i\omega(\Lambda+A)}}{\omega \cosh(u\omega)}, \\ g_n(\Lambda) &= \int_0^{\infty} d\Lambda' R(\Lambda + \Lambda' + 2A) y_{n-1}(\Lambda'). \end{aligned} \quad (A7)$$

To solve these integral equations for $y_n(\Lambda)$, we begin

by defining

$$\tilde{y}_n^\pm(\omega) = \int_{-\infty}^{\infty} d\Lambda \theta_H(\pm\Lambda) y_n(\Lambda) e^{i\omega\Lambda},$$

where $\tilde{y}_n^+(\omega)$ ($\tilde{y}_n(\omega)$) is an analytic function in the upper (lower) half-plane. It is obvious that the Fourier transformation of $y_n(x)$ satisfies the relation $\tilde{y}_n(\omega) = \tilde{y}_n^+(\omega) + \tilde{y}_n^-(\omega)$.

From Eq. (A6) it follows that

$$\tilde{y}_n^+(\omega) \frac{1}{1 + \exp(-2|u||\omega|)} + \tilde{y}_n^-(\omega) = \tilde{g}_n(\omega), \quad (\text{A8})$$

by applying Fourier transformation. We further decompose the denominator $1 + \exp(-2|u||\omega|)$ into a product of two pieces,

$$1 + \exp(-2|u||\omega|) = G^+(\omega)G^-(\omega), \quad (\text{A9})$$

where $G^+(\omega)$ ($G^-(\omega)$) is an analytic function in the upper (lower) half-plane. Then substituting this last equation into Eq. (A8) results in the form

$$\tilde{y}_n^+(\omega)/G^+(\omega) + G^-(\omega)\tilde{y}_n^-(\omega) = G^-(\omega)\tilde{g}_n(\omega). \quad (\text{A10})$$

Furthermore, we decompose $G^-(\omega)\tilde{g}_n(\omega)$ into a sum of two pieces,

$$G^-(\omega)\tilde{g}_n(\omega) = Q_n^+(\omega) + Q_n^-(\omega), \quad (\text{A11})$$

where similarly $Q_n^+(\omega)$ ($Q_n^-(\omega)$) is an analytic function in the upper (lower) half-plane. Then substitution of this last equation into Eq. (A10) gives

$$\tilde{y}_n^+(\omega) = G^+(\omega)Q_n^+(\omega), \quad (\text{A12})$$

$$\tilde{y}_n^-(\omega) = Q_n^-(\omega)/G^-(\omega). \quad (\text{A13})$$

In this way we can work out the Fourier transformation of $y_0(\Lambda)$ and $y_n(\Lambda)$ itself.

To this end, recalling (A11), we firstly decompose $1 + \exp(-2|u||\omega|)$ as

$$\begin{aligned} G^+(\omega) &= G^-(-\omega) \\ &= \frac{\sqrt{2\pi}}{\Gamma(\frac{1}{2} - \frac{i|u|\omega}{\pi})} \left(-\frac{i|u|\omega}{\pi} \right)^{-\frac{i|u|\omega}{\pi}} \exp\left(\frac{i|u|\omega}{\pi} \right), \end{aligned} \quad (\text{A14})$$

where we should note that $\lim_{\omega \rightarrow \infty} G^\pm(\omega) = 1$, along with the special values $G^\pm(0) = \sqrt{2}$ and $G^\pm\left(\pm \frac{i\pi}{2|u|}\right) = \sqrt{\pi/e}$ of these functions.

The decomposition for $G^-(\omega)\tilde{g}_n(\omega)$ in general is subtle, however the leading case $G^-(\omega)\tilde{g}_0(\omega)$ is accessible. We start analysis from the Fourier transformation of $g_0(\Lambda)$,

$$\tilde{g}_0(\omega) = -\mu 2\pi\delta_D(\omega) - \frac{2\pi J_1(\omega) \exp(-i\omega A)}{\omega \cosh(u\omega)}, \quad (\text{A15})$$

where on the rhs the δ_D function could be decomposed as

$$2\pi\delta_D(\omega) = i \left(\frac{1}{\omega + i\epsilon} - \frac{1}{\omega - i\epsilon} \right) \quad (\epsilon \rightarrow +0). \quad (\text{A16})$$

The second term on the rhs is a meromorphic function of ω with poles located at

$$\omega_n = i \frac{\pi}{2|u|} (2n+1) \quad (n \in \mathbf{Z}) \quad (\text{A17})$$

originating from the term $\frac{1}{\cosh(u\omega)}$, implying the decomposition

$$\begin{aligned} \frac{1}{\cosh(u\omega)} &= \chi^+(\omega) + \chi^-(\omega), \\ \chi^+(\omega) &= \frac{i}{|u|} \sum_{n=0}^{\infty} (-1)^n \frac{1}{\omega + \omega_n}, \\ \chi^-(\omega) &= \frac{1}{\cosh(u\omega)} - \frac{i}{|u|} \sum_{n=0}^{\infty} (-1)^n \frac{1}{\omega + \omega_n}, \end{aligned} \quad (\text{A18})$$

where $\chi^+(\omega)$ and $\chi^-(\omega)$ are analytic functions in the upper and lower half-planes, respectively. With the help of Eq. (A18), as for any analytic and bounded function $f^-(\omega)$ in the lower half-plane, the decomposition of $\frac{f^-(\omega)}{\cosh(u\omega)}$ is

$$\begin{aligned} \frac{f^-(\omega)}{\cosh(u\omega)} &= F^+(\omega) + F^-(\omega), \\ F^+(\omega) &= \frac{i}{|u|} \sum_{n=0}^{\infty} (-1)^n \frac{f^-(-\omega_n)}{\omega + \omega_n}, \\ F^-(\omega) &= \frac{f^-(\omega)}{\cosh(u\omega)} - F^+(\omega). \end{aligned} \quad (\text{A19})$$

By virtue of Eqs. (A15) and (A19), we make the following decomposition for $G^-(\omega)\tilde{g}_0(\omega)$,

$$\begin{aligned} Q_0^+(\omega) &= -\frac{i\mu G^-(0)}{\omega + i\epsilon} - q(\omega) \\ Q_0^-(\omega) &= \frac{i\mu G^-(0)}{\omega + i\epsilon} - \frac{2\pi J_1(\omega) \exp(-i\omega A) G^-(\omega)}{\omega \cosh(u\omega)} + q(\omega) \end{aligned} \quad (\text{A20})$$

where $q(\omega) = 4i \sum_{n=1}^{\infty} (-1)^n \frac{G^-(-ih_n) I_1(h_n) \exp(-h_n A)}{(2n+1)(\omega + ih_n)}$, $I_1(z)$ is the first order modified Bessel function, $h_n = \frac{\pi}{2|u|} (2n+1)$, with the series converging only if $A > 1$.

If $A \gg 1$, using Eq. (A12), we have

$$y_0^+(\omega) = G^+(\omega) \left[-\frac{i\mu G^-(0)}{\omega + i\epsilon} - q(\omega) \right]. \quad (\text{A21})$$

Obviously, we know $y(0) = \varepsilon'_1(A) = 0$, which implies

$$0 = y(0) = \lim_{\omega \rightarrow \infty} -i\omega \tilde{y}^+(\omega). \quad (\text{A22})$$

Hereafter we replace $y(\omega)$ with $y_0(\omega)$, which is a reasonable approximation if $A \gg 1$. Therefore Eqs. (A21) and (A22) give rise to

$$\mu = -4 \sum_{n=0}^{\infty} \frac{G^-(-ih_n) I_1(h_n) \exp(-h_n A)}{(2n+1) G^-(0)}. \quad (\text{A23})$$

Since we have obtained a parametric expression for the critical chemical potential, we turn to the expression for the magnetic field. Due to the fact that the phase boundary is determined by $\varepsilon^u(0) = 0$, we thus use Eq. (A1) to determine the magnetic field.

For simplicity, we rewrite Eqs. (A1) and (A2) as

$$\begin{aligned} \varepsilon^u(k) &= -2 \cos k - \mu - 2u - B \\ &+ \int_A^\infty d\Lambda [a_1(\sin k - \Lambda) + a_1(\sin k + \Lambda)] \varepsilon'_1(\Lambda) \\ &- \int_{-\infty}^\infty d\Lambda a_1(\sin k - \Lambda) \varepsilon'_1(\Lambda), \end{aligned} \quad (\text{A24})$$

$$\varepsilon'_1(\Lambda) = \varepsilon_1'^{(0)}(\Lambda) - \int_{-A}^A d\Lambda' a_2(\Lambda - \Lambda') \varepsilon'_1(\Lambda'), \quad (\text{A25})$$

where we have denoted

$$\varepsilon_1'^{(0)}(\Lambda) = -2\mu - 2 \int_{-\pi}^\pi dk \cos^2 k a_1(\sin k - \Lambda). \quad (\text{A26})$$

Substituting Eq. (A25) into the last term on the rhs of Eq. (A24) gives

$$\begin{aligned} \varepsilon^u(k) &= -2 \cos k - \mu - 2u - B \\ &+ \int_0^\infty d\Lambda [s(\Lambda + A - \sin k) + s(\Lambda + A + \sin k)] y(\Lambda) \\ &- \int_{-\infty}^\infty d\Lambda s(\Lambda - \sin k) \varepsilon_1'^{(0)}(\Lambda), \end{aligned} \quad (\text{A27})$$

where we have introduced the function $s(x) = \frac{1}{4|u| \cosh(\frac{\pi x}{2|u|})}$ and made use of the two identities

$$\begin{aligned} \frac{1}{4|u| \cosh(\frac{\pi x}{2|u|})} &= \sum_{n=0}^\infty (-1)^n a_{2n+1}(x), \\ \int_{-\infty}^\infty dy a_n(x-y) a_m(y-z) &= a_{m+n}(x-z). \end{aligned}$$

Substituting the expansion $s(x) = \frac{1}{2|u|} \sum_{n=0}^\infty (-1)^n \exp(-h_n x)$, where $|\pi x/u| < 1$ and Eq. (A26) into Eq. (A27), and after some algebraic manipulations, we arrive at the result

$$\begin{aligned} \varepsilon^u(k) &= -2 \cos k - 2u - B \\ &+ \sum_{n=0}^\infty \frac{(-1)^n}{|u|} \tilde{y}^+(i h_n) \cosh(h_n \sin k) \exp(-h_n A) \\ &+ 2 \int_0^\infty \frac{d\omega J_1(\omega) \cos(\omega \sin k) \exp(-|u|\omega)}{\omega \cosh(u\omega)}, \end{aligned} \quad (\text{A28})$$

Using Eq. (A28) and $\varepsilon^u(0) = 0$ we derive the expression

$$B = -2 + 2|u| + \sum_{n=0}^\infty \frac{(-1)^n}{|u|} \tilde{y}^+(i h_n) \exp(-h_n A)$$

$$+ 2 \int_0^\infty d\omega \frac{J_1(\omega) \exp(-|u|\omega)}{\omega \cosh(u\omega)} \quad (\text{A29})$$

for determining the critical magnetic field. Here we denoted $h_n = \frac{\pi}{2|u|}(2n+1)$. The equation (A29) sets up a relation between the magnetic field and the chemical potential. In summary, the phase boundary between phase IV and V is determined by Eqs. (A23) and (A29) for $A \gg 1$.

B. Derivation of the Equation of State

The derivation of the equation of state is rather involved. Here we sketch the calculations for the terms p^u and p_n^b .

Prior to substituting the dressed energies into the definitions of p^u and p_n^b integrating by parts, we first need to find a suitable form of the TBA equations for this procedure, i.e., (34) and (35). For simplicity in later discussion, we approximate the definition of p_n^b as

$$\begin{aligned} p_n^b &= \int_{-\infty}^\infty \frac{d\Lambda}{\pi} \text{Re} \frac{1}{\sqrt{\Lambda + i n |u|}} \varepsilon_n'^-(\Lambda) \\ &= T \int_{-\infty}^\infty \frac{d\Lambda}{2\pi} \int_{-\pi}^\pi dk a_n(\Lambda - \sin k) \\ &= \int_{-\infty}^\infty d\Lambda \varepsilon_n'^-(\Lambda) \Delta_n(\Lambda) + o\left(\frac{1}{|u|^4}\right), \end{aligned} \quad (\text{B30})$$

where $\Delta_n(\Lambda) = a_n(\Lambda) - \frac{1}{2}b_n(\Lambda) + 2\Lambda^2 b_n(\Lambda)$. In the above equations, we used the abbreviations

$$\begin{aligned} \varepsilon_n'^-(x) &= T \ln \left(1 + e^{-\varepsilon_n'(x)/T} \right), \\ \varepsilon_n^-(x) &= T \ln \left(1 + e^{-\varepsilon_n(x)/T} \right). \end{aligned}$$

To obtain the result (34), regarding the first series of integral terms on the rhs of (17), we expand them in the strong coupling regime as

$$\begin{aligned} &\sum_{n=1}^\infty \int_{-\infty}^\infty d\Lambda a_n(\sin k - \Lambda) \varepsilon_n'^-(\Lambda) \\ &= \sum_{n=1}^\infty \int_{-\infty}^\infty d\Lambda \Delta_n(\Lambda) \varepsilon_n'^-(\Lambda) \times \\ &\quad \frac{a_n(\Lambda) \left\{ 1 + \frac{2\Lambda \sin k - \sin^2 k}{(nu)^2 + \Lambda^2} + \left[\frac{2\Lambda \sin k - \sin^2 k}{(nu)^2 + \Lambda^2} \right]^2 \right\}}{\Delta_n(\Lambda)} + o\left(\frac{1}{|u|^4}\right) \\ &= \sum_{n=1}^\infty p_n^b + \bar{a} + 2\bar{a} \cos^2 k + o\left(\frac{1}{|u|^4}\right), \end{aligned} \quad (\text{B31})$$

where we have inserted (B30) and \bar{a} has been defined in section III.

While for the second series of integral terms, it is easy to see that under the assumption $B/T \gg 1$, these spin-wave contributions are no more than

$-T e^{-2B/T} e^{-\bar{K}} I_0(\bar{K})$, which is accessible through simple iteration of (18). In fact, the spin degree of freedom is frozen here, and thus this term could be neglected in later discussion.

We can rewrite (34) as

$$\varepsilon^u(k) = \varepsilon_0^u(k) - A^u, \quad (\text{B32})$$

where $\varepsilon_0^u(k) = -2 \cos k + 2\bar{a} \cos^2 k$ and $A^u = \mu + 2u + B - \sum_{n=1}^{\infty} p_n^b + \bar{a}$.

Integrating by parts in p^u , we obtain

$$p^u = T \ln \left(1 + e^{(\mu+2u+B-\sum_{n=1}^{\infty} p_n^b + \bar{a}-2)/T} \right) + \frac{1}{\pi} \int_{2\bar{a}-2}^{2\bar{a}+2} \frac{d\varepsilon_0^u k(\varepsilon_0^u)}{1 + e^{\varepsilon_0^u/T/z}}, \quad (\text{B33})$$

where $z = e^{A^u/T}$ and $k(\varepsilon_0^u) = \arccos \left(\frac{1 - \sqrt{1 + 2\bar{a}\varepsilon_0^u}}{2\bar{a}} \right)$ represents the inverse function of $\varepsilon_0^u(k)$. By taking account of $\bar{a} \sim \sum_{n=1}^{\infty} \frac{p_n^b}{(nu)^2}$ for the strong coupling regime, the integral in the above equation can be further simplified,

$$\begin{aligned} & \frac{1}{\pi} \int_{2\bar{a}-2}^{2\bar{a}+2} \frac{d\varepsilon_0^u k(\varepsilon_0^u)}{1 + e^{\varepsilon_0^u/T/z}} = \frac{2}{\pi} \int_{\bar{a}-1}^{\bar{a}+1} dx \frac{k(2x)}{1 + e^{2x/T/z}} \\ & = \frac{2}{\pi} \int_{-1}^1 dx \frac{\arccos(-x)}{1 + e^{2x/T/z}} - \frac{2\bar{a}}{\pi} \int_{-1}^1 \frac{dx x^2 / \sqrt{1-x^2}}{1 + e^{2x/T/z}} \\ & + \frac{2\bar{a}}{1 + e^{2\varepsilon^u(\pi)/T}} + o\left(\frac{1}{|u|^4}\right), \end{aligned} \quad (\text{B34})$$

where we have changed the integration variable $\varepsilon_0^u = 2x$ and then applied Taylor expansion with respect to \bar{a} . See $\varepsilon^u(\pi)$ in section III. The result (38) is therefor achieved.

We then turn to the transformation of $\varepsilon'_n(\Lambda)$. Similar to the treatment for $\varepsilon^u(k)$, we employ Taylor expansion to expand (19) in the strong coupling region, with result

$$\begin{aligned} \varepsilon'_n(\Lambda) &= -2n\mu - a_n(\Lambda) \left[2\pi - \int_{-\pi}^{\pi} dk \cos k \varepsilon^{u-}(k) \right] \\ &- b_n(\Lambda) \left[-\frac{\pi}{2} - \int_{-\pi}^{\pi} dk \cos k \sin^2 k \varepsilon^{u-}(k) \right] \\ &+ \sum_{m=1}^{\infty} T_{nm} * \varepsilon'_m(\Lambda) + o\left(\frac{1}{|u|^4}\right), \end{aligned} \quad (\text{B35})$$

where the integral terms in the brackets are denoted as d_1 and d_2 , respectively. Here d_1 and d_2 can be calculated via integration by parts, similar to that done for p^u above, see the explicit expressions in section III. With respect to the convolution term, due to the condition of low density, the cut-off of the dressed energy $\varepsilon'_n(\Lambda)$ is small, thus in general we can make the approximations

$$\begin{aligned} & \int_{-\infty}^{\infty} d\Lambda' a_p(\Lambda - \Lambda') \varepsilon'_q(\Lambda') \\ &= \int_{-\infty}^{\infty} d\Lambda' a_p(\Lambda') \varepsilon'_q(\Lambda') \end{aligned}$$

$$-\Lambda^2 \int_{-\infty}^{\infty} d\Lambda' b_p(\Lambda') \varepsilon'_q(\Lambda') + o\left(\frac{1}{|u|^4}\right), \quad (\text{B36})$$

which results in Eq. (35) in the main text.

We next rewrite (35) as

$$\varepsilon'_n(\Lambda) = D_n \left(\frac{\Lambda}{n|u|} \right)^2 - A_n^b, \quad (\text{B37})$$

where $A_n^b = 2n\mu - \eta_n + \frac{d_1}{\pi n|u|} + \frac{d_2}{2\pi(n|u|)^3}$ and D_n was defined in section III. section III is arrived at by substituting the above equation into the definition of p_n^b and integrating by parts.

Lastly, \bar{a} , $\xi_p^m = T \int_{-\infty}^{\infty} d\Lambda' a_p(\Lambda') \varepsilon'_m(\Lambda')$ and $\phi_p^m = T \int_{-\infty}^{\infty} d\Lambda' b_p(\Lambda') \varepsilon'_m(\Lambda')$ are calculated in a similar way.

C. Some constants in the scaling functions

The constants used in the scaling forms for the phase transition (II-IV) are given explicitly by

$$\begin{aligned} \lambda_1 &= -\frac{2\sqrt{|u|}(1 - q_{c4}/\pi)}{\sqrt{2\pi - q_{c4}^3/3}}, \\ \lambda_2 &= \frac{(1 - q_{c4}/\pi)q_{c4}/\pi}{\sqrt{|u|}\sqrt{2\pi - q_{c4}^3/3}}, \\ \kappa_{b4} &= \gamma, \quad m_{b4} = \frac{1}{2}\gamma, \\ \kappa_{b4} &= \gamma' \left(1 + \frac{4}{\sqrt{\pi}} \tau^{\frac{1}{2}} \tilde{f}_{\frac{1}{2}} + \frac{6}{\pi} \tau \tilde{f}_{\frac{1}{2}}^2 + \frac{5}{\pi^{\frac{3}{2}}} \tau^{\frac{3}{2}} \tilde{f}_{\frac{1}{2}}^3 - \frac{2}{\sqrt{\pi}} \tau^{\frac{3}{2}} \tilde{f}_{\frac{3}{2}} \right), \\ \lambda_3 &= -\frac{4\sqrt{|u|}(1 - q_{c4}/\pi)}{\sqrt{2\pi - q_{c4}^3/3}}, \\ \chi_{b4} &= \frac{1}{2}\gamma' + \frac{2\delta\gamma' - (1-\gamma)\delta'}{|u|\sqrt{\pi}} \left(\tau^{\frac{1}{2}} \tilde{f}_{\frac{1}{2}} + \frac{1}{2\sqrt{\pi}} \tau \tilde{f}_{\frac{1}{2}}^2 + \frac{1}{4\pi} \tau^{\frac{3}{2}} \tilde{f}_{\frac{1}{2}}^3 \right. \\ &\quad \left. - \tau^{\frac{3}{2}} \tilde{f}_{\frac{3}{2}} \right), \\ \lambda_4 &= -\frac{2(q_{c4}/\pi)^2(1 - q_{c4}/\pi)}{\sqrt{|u|^3}\sqrt{2\pi - q_{c4}^3/3}}. \end{aligned} \quad (\text{C38})$$

Here the parameter $q_{c4} = \sqrt{B+2-2\sqrt{1+u^2}} + \frac{1}{3\pi|u|}(B+2-2\sqrt{1+u^2})$.

The constants used in the scaling forms for the phase transition (V-IV) are given explicitly by

$$\begin{aligned} \kappa_{b5} &= -\frac{2}{\sqrt{\pi}} \tau^{\frac{1}{2}} \tilde{f}_{\frac{1}{2}} - \frac{1}{\pi} \tau \tilde{f}_{\frac{1}{2}}^2 - \frac{1}{2\pi^{\frac{3}{2}}} \tau^{\frac{3}{2}} \tilde{f}_{\frac{1}{2}}^3 + \frac{1}{\sqrt{\pi}} \tau^{\frac{3}{2}} \tilde{f}_{\frac{3}{2}}, \\ \lambda_5 &= -\frac{1}{2\sqrt{\pi}} \left(1 - \frac{4}{\pi} \sqrt{1 + \frac{2\pi|u|\tilde{\mu}_{c5}}{2\pi - q_{c5}^3/3}} \right), \\ \lambda_6 &= -\frac{1}{2\sqrt{\pi}} \left(1 - \frac{8}{\pi} \sqrt{1 + \frac{2\pi|u|\tilde{\mu}_{c5}}{2\pi - q_{c5}^3/3}} \right) \\ \kappa_{b5} &= -\frac{(1-\gamma)\tilde{f}_{-\frac{1}{2}}}{D_0\tau^{\frac{1}{2}}} \left(\frac{4}{\sqrt{\pi}} + \frac{6}{\pi} \tau^{\frac{1}{2}} \tilde{f}_{\frac{1}{2}} + \frac{6}{\pi^{\frac{3}{2}}} \tau \tilde{f}_{\frac{1}{2}}^2 \right) \end{aligned}$$

$$-\frac{7}{4\pi}\tau^{\frac{3}{2}}\tilde{f}_{\frac{3}{2}} + \frac{5}{\pi^2}\tau^{\frac{3}{2}}\tilde{f}_{\frac{3}{2}}^3), \quad (\text{C39})$$

where $\tilde{\mu}_{c5} \approx 2|u| - B - 2 + \frac{8\sqrt{2}}{3\pi|u|\alpha_1} (2\sqrt{1+u^2} - B - 2)^{\frac{3}{2}}$ and $q_{c5} = \sqrt{\tilde{\mu}_{c5} + 2u + B + 2}$.

D. Explicit forms of the additivity rules

The vectorial forms of Eqs. (76) and (77) are accessible by expanding the rescaled TBA equations in terms of

$$\mathbf{A}_{(1)}^1(\tilde{y}_c) = \frac{2}{\pi} \begin{bmatrix} 1 & 0 & \cdots \\ -1 & 0 & \cdots \\ \vdots & & \end{bmatrix} \tilde{y}_c,$$

$$\mathbf{A}_{(3)}^1(\tilde{y}_c) = \frac{2}{\pi} \begin{bmatrix} -\frac{1}{3} & \frac{1}{3} & \cdots \\ 2 & \frac{1}{3} & \cdots \\ \vdots & & \end{bmatrix} \tilde{y}_c^3,$$

Next, the partial derivatives of Eqs. (76) and (77) read

$$\frac{\partial \tilde{\varepsilon}^1}{\partial \tilde{\mu}} = \frac{\partial \tilde{V}^1}{\partial \tilde{\mu}} - \mathbf{A}^1(\tilde{\Lambda}_c) \frac{\partial \tilde{\varepsilon}^2}{\partial \tilde{\mu}}, \quad (\text{D43})$$

$$\frac{\partial \tilde{\varepsilon}^2}{\partial \tilde{\mu}} = \tilde{V}^2 - \mathbf{A}^1(\tilde{k}_c) \frac{\partial \tilde{\varepsilon}^1}{\partial \tilde{\mu}} - \mathbf{A}^2(\tilde{\Lambda}_c) \frac{\partial \tilde{\varepsilon}^2}{\partial \tilde{\mu}}. \quad (\text{D44})$$

With the help of the explicit forms of $\mathbf{A}^n(\tilde{y}_c)$, i.e., (D41) and (D42), we can obtain Eq. (82), which relates the densities and the cutoffs. Together with Eq. (79), we then obtain the relation between the densities and the effective chemical potentials (90) and (91).

On this basis, we now proceed to derive the explicit expressions for the effective compressibility and susceptibility in terms of densities of bound pairs and excess fermions. Apparently, the densities of bound pairs and excess fermions rely on the chemical potential and the magnetic field, and vice versa, which in fact indicates under fixed magnetic field one could obtain the following results through the total derivatives,

$$\kappa_1 = \left(\frac{\partial n_1}{\partial \mu_1} \right)_B = \frac{dn_1}{d\mu}, \quad \kappa_2 = 2 \left(\frac{\partial n_2}{\partial \mu_2} \right)_B = \alpha_1 \frac{dn_2}{d\mu}, \quad (\text{D45})$$

where we keep $dB = \frac{\partial B}{\partial n_1} dn_1 + \frac{\partial B}{\partial n_2} dn_2 = 0$. Thus we have

$$\frac{dn_1}{d\mu} = \frac{1}{J} \left(\frac{\partial B}{\partial n_2} \right)_{n_1}, \quad \frac{dn_2}{d\mu} = -\frac{1}{J} \left(\frac{\partial B}{\partial n_1} \right)_{n_2}. \quad (\text{D46})$$

Here the Jacobian determinant

$$J = \left(\frac{\partial \mu}{\partial n_1} \right)_{n_2} \left(\frac{\partial B}{\partial n_2} \right)_{n_1} - \left(\frac{\partial B}{\partial n_1} \right)_{n_2} \left(\frac{\partial \mu}{\partial n_2} \right)_{n_1}$$

$\{k^{2n}\}$ and $\{\Lambda^{2n}\}$ ($n = 0, 1, 2, \dots$). We here give the explicit expression for the matrix $\mathbf{A}^n(\tilde{y}_c)$ ($n = 1, 2$) with the elements

$$\{\mathbf{A}^n(\tilde{y}_c)\}_{jl} = \frac{2}{\pi} \sum_{0 \leq j \leq i < \infty} \frac{(-1)^i C_{2i}^{2j} \tilde{y}_c^{2i-2j+2l+1}}{n^{2i+1}(2i-2j+2l+1)}, \quad (\text{D40})$$

with $j, l = 0, 1, 2, \dots$. Thus the first two orders of $\mathbf{A}_{(q)}^n(\tilde{y}_c)$ are written as

$$\mathbf{A}_{(1)}^2(\tilde{y}_c) = \frac{1}{\pi} \begin{bmatrix} 1 & 0 & \cdots \\ -\frac{1}{4} & 0 & \cdots \\ \vdots & & \end{bmatrix} \tilde{y}_c, \quad (\text{D41})$$

$$\mathbf{A}_{(3)}^2(\tilde{y}_c) = \frac{1}{\pi} \begin{bmatrix} -\frac{1}{12} & \frac{1}{3} & \cdots \\ \frac{1}{8} & -\frac{1}{12} & \cdots \\ \vdots & & \end{bmatrix} \tilde{y}_c^3. \quad (\text{D42})$$

$$= -\frac{\alpha_1}{2} \left[\left(\frac{\partial \mu_1}{\partial n_1} \right)_{n_2} \left(\frac{\partial \mu_2}{\partial n_2} \right)_{n_1} - \left(\frac{\partial \mu_2}{\partial n_1} \right)_{n_2} \left(\frac{\partial \mu_1}{\partial n_2} \right)_{n_1} \right], \quad (\text{D47})$$

where we have used Eqs. (73) and (74).

Similarly, the magnetic field is dependent on the effective chemical potentials while the latter is dependent on densities of bound pairs and excess fermions. Therefore by application of chain rule we have

$$\left(\frac{\partial B}{\partial n_1} \right)_{n_2} = \left(\frac{\partial \mu_1}{\partial n_1} \right)_{n_2} - \frac{\alpha_1}{2} \left(\frac{\partial \mu_2}{\partial n_1} \right)_{n_2},$$

$$\left(\frac{\partial B}{\partial n_2} \right)_{n_1} = \left(\frac{\partial \mu_1}{\partial n_2} \right)_{n_1} - \frac{\alpha_1}{2} \left(\frac{\partial \mu_2}{\partial n_2} \right)_{n_1}. \quad (\text{D48})$$

It is obvious that once the explicit expression of μ_r in terms of n_s ($r, s = 1, 2$) is known, our goal of the effective compressibilities is easy to achieve. We use Eqs. (79) and (80) and section V to derive

$$\mu_1 = \pi^2 n_1^2 \left[1 + 2 \left(\frac{2n_2}{|u|} \right) + 3 \left(\frac{2n_2}{|u|} \right)^2 \right] + \frac{4\pi^2 \alpha_1}{3\beta_1^3 |u|} n_2^3 \left[1 + 3 \frac{2n_1 + n_2}{\beta_1 |u|} \right], \quad (\text{D49})$$

$$\mu_2 = \frac{\pi^2 n_2^2}{\beta_1^2} \left[1 + 2 \frac{2n_1 + n_2}{\beta_1 |u|} + 3 \left(\frac{2n_1 + n_2}{\beta_1 |u|} \right)^2 \right] + \frac{4\pi^2}{3\alpha_1 |u|} n_1^3 \left[1 + 3 \left(\frac{2n_2}{|u|} \right) \right] + \frac{2\pi^2}{3\beta_1^3 |u|} n_2^3 \left[1 + 3 \frac{2n_1 + n_2}{\beta_1 |u|} \right], \quad (\text{D50})$$

and thus

$$\begin{aligned}
\kappa_1 &= \frac{\pi^2}{J} \left[-\frac{\alpha_1 n_2}{\beta_1^2} - \frac{4\alpha_1 n_1 n_2}{|u|\beta_1^3} + \frac{4n_1^2}{|u|} - \frac{4n_1^3}{u^2} + \frac{24n_1^2 n_2}{u^2} \right. \\
&\quad \left. - \frac{12\alpha_1 n_1^2 n_2}{u^2 \beta_1^4} + \frac{6\alpha_1 n_2^3}{u^2 \beta_1^4} \right], \\
\kappa_2 &= -\frac{2\alpha_1 \pi^2}{J} \left[n_1 - \frac{n_1^2}{|u|} + \frac{4n_1 n_2}{|u|} - \frac{6n_1^2 n_2}{u^2} - \frac{\alpha_1 n_2^2}{u\beta_1^3} \right. \\
&\quad \left. + \frac{12n_1 n_2^2}{u^2} - \frac{6\alpha_1 n_1 n_2^2}{u^2 \beta_1^4} \right], \\
J &= -\frac{2\pi^4 \alpha_1}{\beta_1^2} n_1 n_2 \left[1 + \frac{4n_1}{|u|\beta_1} + \frac{12n_1^2}{u^2 \beta_1^2} + \frac{4n_2}{|u|} + \frac{4n_2}{|u|\beta_1} \right. \\
&\quad \left. + \frac{24n_1 n_2}{u^2 \beta_1^2} + \frac{8n_1 n_2}{u^2 \beta_1} + \frac{12n_2^2}{u^2} + \frac{10n_2^2}{u^2 \beta_1^2} + \frac{16n_2^2}{u^2 \beta_1} \right].
\end{aligned} \tag{D51}$$

The situation for effective susceptibilities is rather simple. With fixed total particle density, one confirms that

$dn_1 + 2dn_2 = 0$, and thus the total derivative of the effective chemical potentials with respect to n_r ($r = 1, 2$) is

$$\begin{aligned}
d\mu_1 &= \left[\left(\frac{\partial \mu_1}{\partial n_1} \right)_{n_2} - \frac{1}{2} \left(\frac{\partial \mu_1}{\partial n_2} \right)_{n_1} \right] dn_1, \\
d\mu_2 &= -2 \left[\left(\frac{\partial \mu_2}{\partial n_1} \right)_{n_2} - \frac{1}{2} \left(\frac{\partial \mu_2}{\partial n_2} \right)_{n_1} \right] dn_2.
\end{aligned} \tag{D53}$$

After some algebraic manipulations we then obtain

$$\begin{aligned}
\bar{\chi}_1 &= 1 / \left(\frac{\partial \mu_1}{\partial n_1} - \frac{1}{2} \frac{\partial \mu_1}{\partial n_2} \right), \\
\bar{\chi}_2 &= -1 / \left(\frac{\partial \mu_2}{\partial n_1} - \frac{1}{2} \frac{\partial \mu_2}{\partial n_2} \right),
\end{aligned} \tag{D54}$$

which together with Eqs. (D49) and (D50) result in

$$\begin{aligned}
\bar{\chi}_1 &= \frac{1/(2\pi^2)}{n_1 - \frac{n_1^2}{|u|} + \frac{4n_1 n_2}{|u|} - \frac{6n_1^2 n_2}{u^2} - \frac{\alpha_1 n_2^2}{|u|\beta_1^3} + \frac{12n_1 n_2^2}{u^2} - \frac{6\alpha_1 n_1 n_2^2}{u^2 \beta_1^4}}, \\
\bar{\chi}_2 &= \frac{1/\pi^2}{\frac{n_2}{\beta_1^2} - \frac{4n_1^2}{|u|\alpha_1} + \frac{4n_1^3}{u^2 \alpha_1} + \frac{4n_1 n_2}{|u|\beta_1^3} - \frac{24n_1^2 n_2}{u^2 \alpha_1} + \frac{12n_1^2 n_2}{u^2 \beta_1^4} - \frac{6n_2^3}{u^2 \beta_1^4}}.
\end{aligned} \tag{D55}$$

* xiwen.guan@anu.edu.au

¹ J. Hubbard, J. Proc. R. Soc. A **276**, 237 (1963); *ibid* **281** 401 (1964).
² C. N. Yang, Phys. Rev. Lett. **19**, 1312 (1967).
³ R. J. Baxter, Ann. Phys. (N.Y.) **70**, 193 (1972).
⁴ E. H. Lieb and F. Y. Wu, Phys. Rev. Lett. **20**, 1445 (1968).
⁵ F. H. L. Essler, H. Frahm, F. Göhmann, A. Klümper and V. E. Korepin, *The One-Dimensional Hubbard Model* (Cambridge University Press, Cambridge, 2005).
⁶ M. Takahashi, Prog. Theo. Phys. **42**, 1098 (1969); *ibid* **43**, 860 (1970); *ibid* **43**, 1619 (1970).
⁷ M. Takahashi, Prog. Theo. Phys. **45**, 756 (1971).
⁸ H. Shiba, Phys. Rev. B **6**, 930 (1972).
⁹ V. Ya. Krivnov and A. A. Ovchinnikov, Zh. Eksp. Teor. Fiz. **67**, 1568 (1974).
¹⁰ T. Usuki, N. Kawakami and A. Okiji, Phys. Lett. A **135**, 476 (1989).
¹¹ F. Woynarovich and K. Penc, Z. Phys. B **85**, 269 (1991).
¹² C. F. Coll, Phys. Rev. B **9**, 2150 (1974).
¹³ A. A. Ovchinnikov, Sov. Phys. JETP **30**, 1160 (1970).
¹⁴ F. Woynarovich, J. Phys. C **15**, 85 (1982); *ibid* **15**, 97 (1982); *ibid* **16**, 5293 (1983).
¹⁵ A. Klümper, A. Schadschneider and J. Zittartz, Z. Phys. B **78**, 99 (1990).
¹⁶ T. Deguchi, F. H. L. Essler, F. Göhmann, A. Klümper, V.

E. Korepin and K. Kusakabe, Phys. Rep. **331**, 197 (2000).
¹⁷ F. Woynarovich, J. Phys. C **16**, 6593 (1983).
¹⁸ F. H. L. Essler and V. E. Korepin, Phys. Rev. Lett. **72**, 908 (1994).
¹⁹ F. H. L. Essler and V. E. Korepin, Nucl. Phys. B **426**, 505 (1994).
²⁰ M. Takahashi, Prog. Theo. Phys. **47**, 69 (1972).
²¹ M. Takahashi, Prog. Theo. Phys. **52**, 103 (1974).
²² K.-J.-B. Lee and P. Schlottmann, Phys. Rev. B **38**, 11566 (1988).
²³ N. Kawakami, T. Usuki and A. Okiji, Phys. Lett. A **137**, 287 (1989); T. Usuki, N. Kawakami and A. Okiji, J. Phys. Soc. Japan **59**, 1357 (1990).
²⁴ P. D. Sacramento, J. Phys. C **7**, 143 (1995).
²⁵ H. Frahm and V. E. Korepin, Phys. Rev. B **42**, 10553 (1990); *ibid* **43**, 5653 (1991).
²⁶ F. Woynarovich and H. P. Eckle, J. Phys. A **20**, L443 (1987); F. Woynarovich, J. Phys. A **22** 4243 (1989).
²⁷ M. Ogata and H. Shiba, Phys. Rev. B **41**, 2326 (1990); M. Ogata, T. Sugiyama and H. Shiba, Phys. Rev. B **43**, 8401 (1991).
²⁸ A. Parola and S. Sorella, Phys. Rev. Lett. **64**, 1831 (1990); Phys. Rev. Lett. **45**, 13156 (1992); Phys. Rev. B **57**, 6444 (1997).
²⁹ K. Penc, F. Mila and H. Shiba, Phys. Rev. Lett. **75**, 894

- (1995); K. Penc, K. Hallberg, F. Mila and H. Shiba, Phys. Rev. Lett. **77**, 1390 (1996); Phys. Rev. B **55**, 15475 (1997).
- ³⁰ F. Göhmann, A. R. Its and V. E. Korepin, Phys. Lett. A **249**, 117 (1998); F. Göhmann and V. E. Korepin, Phys. Lett. A **260**, 516 (1999).
- ³¹ E. Jeckelmann, F. Gebhard and F. H. L. Essler, Phys. Rev. Lett. **85**, 3910 (2000); F. H. L. Essler and A. M. Tsvelik, Phys. Rev. B **65**, 115117 (2002); D. Controzzi and F. H. L. Essler, Phys. Rev. B **66**, 165112 (2002); B. Doyon and S. Lukyanov, Nucl. Phys. B **644**, 451 (2002); F. H. L. Essler and A. M. Tsvelik, Phys. Rev. Lett. **90**, 126401 (2003).
- ³² N. M. Bogoliubov and V. E. Korepin, Mod. Phys. Lett. B **1**, 349 (1988); Teor. i Mat. Fiz. **82**, No. 3, 331 (1990); Int. J. Mod. Phys. B **3**, 427 (1994).
- ³³ A. E. Feiguin, and F. Heidrich-Meisner, Phys. Rev. B **76**, 220508(R) (2007); A. Lüscher, R. M. Noack and A. M. Läuchli, Phys. Rev. A **78**, 013637 (2008); M. Rizzi, M. Polini, M. A. Cazalilla, M. P. Tosi and R. Fazio, Phys. Rev. B **77**, 245105 (2008); M. Tezuka and M. Ueda, Phys. Rev. Lett. **100**, 110403 (2008); M. Tezuka and M. Ueda, New J. Phys. **12**, 055029 (2010).
- ³⁴ G. G. Batrouni, M. H. Huntley, V.G. Rousseau and R. T. Scalettar, Phys. Rev. Lett. **100**, 116405 (2008); S. K. Baur, J. Shumway and E. J. Mueller, Phys. Rev. A **81**, 033628 (2010); M. J. Wolak, V. G. Rousseau, C. Miniatura, B. Gémaud, R. T. Scalettar and G. G. Batroun, Phys. Rev. A **82**, 013614 (2010).
- ³⁵ S. Cheng, Y.-Z. Jiang, Y.-C. Yu, M. T. Batchelor and X.-W. Guan, Nucl. Phys. B **929**, 353 (2018).
- ³⁶ A. Klümper and R.Z. Bariev, Nucl. Phys. B **458**, 623 (1996); G. JüKttner, A. Klümper and J. Suzuki, Nucl. Phys. B **522**, 471 (1998).
- ³⁷ C. N. Yang and C. P. Yang, J. Math. Phys. **10**, 1115 (1969).
- ³⁸ T. Koma, Prog. Theor. Phys. **78**, 1213 (1987); *ibid* **81**, 783 (1989).
- ³⁹ J. L. Cardy, J. Phys. A **17**, L385 (1984); Nucl. Phys. B **270** 186, (1986).
- ⁴⁰ H. W. Blöte, J. L. Cardy and M. P. Nightingale, Phys. Rev. Lett. **56**, 742 (1986).
- ⁴¹ I. Affleck, Phys. Rev. Lett. **56**, 746 (1986).
- ⁴² A. A. Belavin, A. M. Polyakov and A. B. Zamolodchikov, Nucl. Phys. B **241**, 333 (1984).
- ⁴³ E. Zhao and W. Vincent Liu, Phys. Rev. A **78**, 063605 (2008).
- ⁴⁴ J. Kajala, F. Massel and P. Törmä, Phys. Rev. A **84**, 041601 (R) (2011).
- ⁴⁵ A. Singha, M. Gibertini, B. Karmakar, S. Yuan, M. Polini, G. Vignale, M. I. Katsnelson, A. Pinczuk, L. N. Pfeiffer, K. W. West and V. Pellegrini, Science **332**, 1176 (2011).
- ⁴⁶ R. A. Hart, P. M. Duarte, T.-L. Yang, X. Liu, T. Paiva, E. Khatami, R. T. Scalettar, N. Trivedi, D. A. Huse and R. G. Hulet, Nature **519**, 211 (2015).
- ⁴⁷ D. Greif, M. F. Parsons, A. Mazurenko, C. S. Chiu, S. Blatt, F. Huber, G. Ji and M. Greiner, Science **351**, 953 (2016).
- ⁴⁸ M. F. Parsons, A. Mazurenko, C. S. Chiu, G. Ji, D. Greif and M. Greiner, Science **353**, 1253 (2016).
- ⁴⁹ L. W. Cheuk, M. A. Nichols, K. R. Lawrence, M. Okan, H. Zhang, E. Khatami, N. Trivedi, T. Paiva, M. Rigol and M. W. Zwierlein, Science **353**, 1260 (2016).
- ⁵⁰ M. Boll, T. A. Hilker, G. Salomon, A. Omran, J. Nespolo, L. Pollet, I. Bloch and C. Gross, Science **353**, 1257 (2016).
- ⁵¹ R. Zhang, Y. Cheng, H. Zhai and P. Zhang, Phys. Rev. Lett. **115**, 135301 (2015).
- ⁵² A. Mazurenko, C. S. Chiu, G. Ji, M. F. Parsons, M. Kanász-Nagy, R. Schmidt, F. Grusdt, E. Demler, D. Greif and M. Greiner, Nature **545**, 462 (2017).
- ⁵³ Y. Kono, T. Sakakibara, C. P. Aoyama, C. Hotta, M. M. Turnbull, C. P. Landee and Y. Takano, Phys. Rev. Lett. **114**, 037202 (2015).
- ⁵⁴ C. Krellner, S. Lausberg, A. Steppke, M. Brando, L. Pedrero, H. Pfau, S. Tencé, H. Rosner, F. Steglich and C. Geibel, New J. Phys. **13**, 103014 (2011).
- ⁵⁵ J. M. P. Carmelo, P. Horsch and A. A. Ovchinnikov, Phys. Rev. B **45**, 7899 (1992).
- ⁵⁶ V. R. Shaginyan, V. A. Stephanovich, K. G. Popov, E. V. Kirichenko and S. A. Artamonov, Ann. Phys. (Berlin) **528**, 483 (2016).
- ⁵⁷ S. Cheng, Y.-Z. Jiang, M. T. Batchelor and X.-W. Guan, “FFLO correlation and free fluids in the one-dimensional attractive Hubbard model”, arXiv:1708.07776.
- ⁵⁸ T. Giamarchi, *Quantum Physics in one dimension* (Oxford University Press, Oxford, 2004).
- ⁵⁹ K. A. Matveev and A. Furusaki, Phys. Rev. Lett. **101**, 170403 (2008).
- ⁶⁰ Y.-C. Yu, Y.-Y. Chen, H.-Q. Lin, R. A. Roemer and X.-W. Guan, Phys. Rev. B **94**, 195129 (2016).
- ⁶¹ M. P. A. Fisher, P. B. Weichman, G. Grinstein and D. S. Fisher, Phys. Rev. B **40**, 546 (1989).
- ⁶² The sound velocity here is accessible by using the formula $v_r = \sqrt{\frac{L}{m_p n_r \tau} \frac{\partial^2 E_r}{\partial L^2}}$, where the particle mass has been rescaled as $m_p = \frac{1}{2}$ and $E_r = e_r L$. See e_r in Eqs. (85) and (86).
- ⁶³ S. Sachdev, *Quantum Phase Transitions* (Cambridge University Press, Cambridge, 1999).
- ⁶⁴ Q. Zhou and T.-L. Ho, Phys. Rev. Lett. **105**, 245702 (2010).
- ⁶⁵ K. R. A. Hazzard and E. J. Mueller, Phys. Rev. A **84**, 013604 (2011).
- ⁶⁶ B. Yang, Y.-Y. Chen, Y.-G. Zheng, H. Sun, H.-N. Dai, X.-W. Guan, Z.-S. Yuan and J.-W. Pan, Phys. Rev. Lett. **119**, 165701 (2017)
- ⁶⁷ F. He, Y.-Z. Jiang, Y.-C. Yu, H.-Q. Lin and X.-W. Guan, arXiv:1702.05903.
- ⁶⁸ A. V. Rozhkov, Phys. Rev. Lett. **112**, 106403 (2014).
- ⁶⁹ A. G. Lebed, Phys. Rev. Lett. **115**, 157001 (2015).